Mario Lucian Vladut Tino

Voltage-mode control of a three-level buck converter operating in discontinuous conduction mode.

Undergraduate thesis project

Supervised by Dr. Carlos Olalla

Electrical Engineering & Electronics, Industrial and Automatic Engineering dual degree

UNIVERSITAT ROVIRA I VIRGILI

Tarragona

2022/2023

Index

1. Introduction 4
   1.1 Background of the converter 4
   1.2 Goal 5
2. Study of the converter 5
   2.1 Switches commutation 6
   2.2 Conduction modes 11
      2.2.1 Continuous conduction mode (CCM) 12
      2.2.2 Discontinuous conduction mode (DCM) 14
   2.3 Converter's output 15
      2.3.1 Matrix M 21
      2.3.2 Steady state model 23
      2.3.3 Dynamic model 25
3. Simulation 28
   3.1 Steady state model simulation 28
   3.2 Dynamic model simulation 31
4. Voltage-mode control 34
5. Prototype 39
   5.1 Prototype testing 40
      5.1.1 Current probe adjustment 41
      5.1.2 Measurements 43
         5.1.2.1Output 43
            5.1.2.1.1Five percent of duty cycle 43
            5.1.2.1.2Ten percent of duty cycle 44
            5.1.2.1.3Fifteen percent of duty cycle 45
            5.1.2.1.4Twenty percent of duty cycle 47
         5.1.2.2MOSFET's gate to source voltage 49
            5.1.2.2.1Five percent of duty cycle 49
            5.1.2.2.2Ten percent of duty cycle 50
            5.1.2.2.3Fifteen percent of duty cycle 51
            5.1.2.2.420% of duty cycle 51
         5.1.2.3Flying capacitor's voltage 52
            5.1.2.3.1Five percent o duty cycle 52
            5.1.2.3.210% of duty cycle 52
            5.1.2.3.315% of duty cycle 53
            5.1.2.3.4Twenty percent of duty cycle 54
6. 3-level buck converter vs conventional buck converter 55
7. Conclusions 57
8. Annex 58

1. Introduction

Currently, there is an economic, political and social impulse to lead an evolution path towards cheaper, more reliable and smaller converters. In order to achieve this, there is the need to emphasize the work being done in today's day in reducing the inductance and output capacitance of the canonical converters, this does not only reduce the size of the converter itself, but also exploits the opportunity to obtain faster responses when working in closed loop configurations involving an improve in dynamic performance as well.

Another aspect to consider, is the environmental implication, the fact that there is a possibility of reducing significantly the size of the converters, implies the reduction of materials being used meaning less pollution overall.

1.1 Background of the converter

The key features of this converter are the reduction of the potential difference across the switches and diodes, lower switching losses, and a decrease in the voltage being applied to the inductor and capacitor.

This multilevel topology is applicable to other canonical converters. This implies a long-term advantage when it comes to accomplish a sustainable outcome, since a highly similar output compared to conventional converters can be achieved, with the advantage of using smaller inductors and capacitors reducing the size of the converters overall.

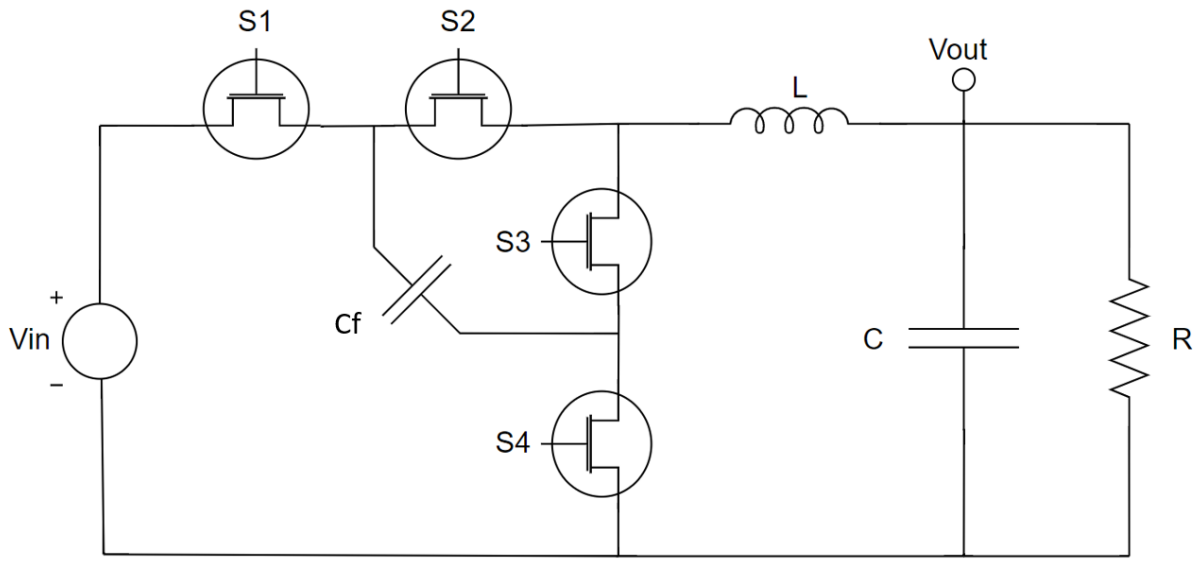

Figure 1: 3-level buck converter

1.2 Goal

The goal of this thesis is to analyse the behaviour of a 3-level Buck converter when working in discontinuous conduction mode (DCM), with the implementation of a voltage control loop. For this, a steady state model and a dynamic model needs to be obtained in order to be able to design the voltage-mode control. Another goal is to build a fully working prototype and to run a series of tests to verify that it is indeed working properly.

In this thesis the DCM behaviour has been analysed, since DCM the switch current always starts from zero (no stored energy) so this implies a lower switching dissipation, therefore more efficient, the downside is that the current peak needs to be higher in order to give enough energy to the output.

2. Study of the converter

The converter has a flying capacitor which its purpose is to lower the voltage that arrives to the filter, depending on how many levels the capacitor has, a different number of flying capacitors will be needed, when dealing with a multilevel converter, the number of flying capacitors that should be used is equal to the number of desired levels, minus one.

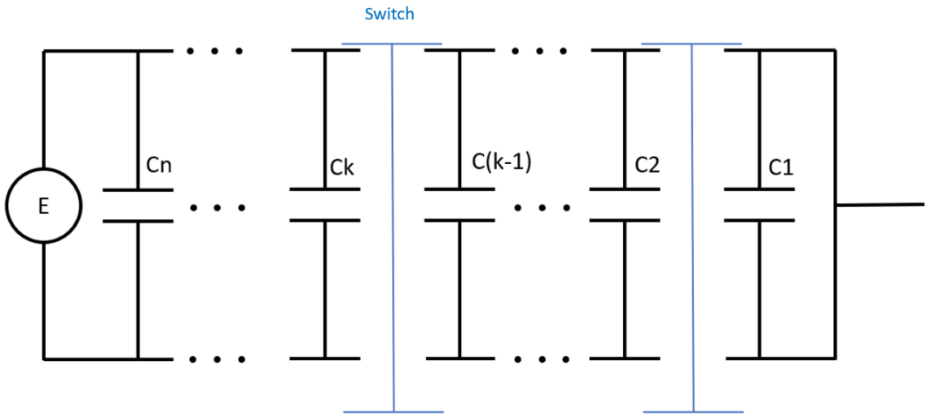

Figure 2: Multilevel commutation

$$V_{Ck} \equiv voltage\ across\ the\ capacitor\ C_k$$

$$V_{Ck} = k \cdot \frac{V}{N}$$

Where:

$$k \equiv number\ of\ the\ capacitor$$

$$k = 1,2 \dots (N-1)$$

$$N \equiv number\ of\ desired\ levels$$

The voltage being applied to the switch (when it's OFF), depends on the capacitor Ck and the previous capacitor C_{k-1}:

$$V_{off\_k} = k \cdot \frac{V}{N} - (k-1) \cdot \frac{V}{N} = \frac{V}{N} \quad \textbf{(1)}$$

It can be appreciated how there is a notorious decrease in the potential difference across the switches thanks to this multilevel topology, the greater the number of levels being used, the greater the decrease of this potential difference.

In this thesis, the focus of the study is a 3-level Buck converter. It is essential to emphasize that the voltage across the flying capacitor is exactly half of the input voltage. This has been demonstrated in

2.1 Switches commutation

The number of pair of switches needed goes according to the number of desired levels.

$$N \equiv number\ of\ desired\ levels$$

There will be the need of N-1 pairs of switches. In order to control them, there will be as many carrier waves as pair of switches.

The switches will commute using a phase-shifted multi-carrier pulse-width modulator (PSMC-PWM), as the name implies, the carrier waves will be phase shifted. They will be shifted by:

$$\frac{T_s}{N-1} \qquad T_s \equiv carrier\ wave\ period \quad \textbf{(2)}$$

As in this thesis a 3-level Buck converter is being studied, there will be 2 pairs of switches and 2 carrier waves that will be phase shifted $\frac{T_s}{2}$, in other words, 180º.

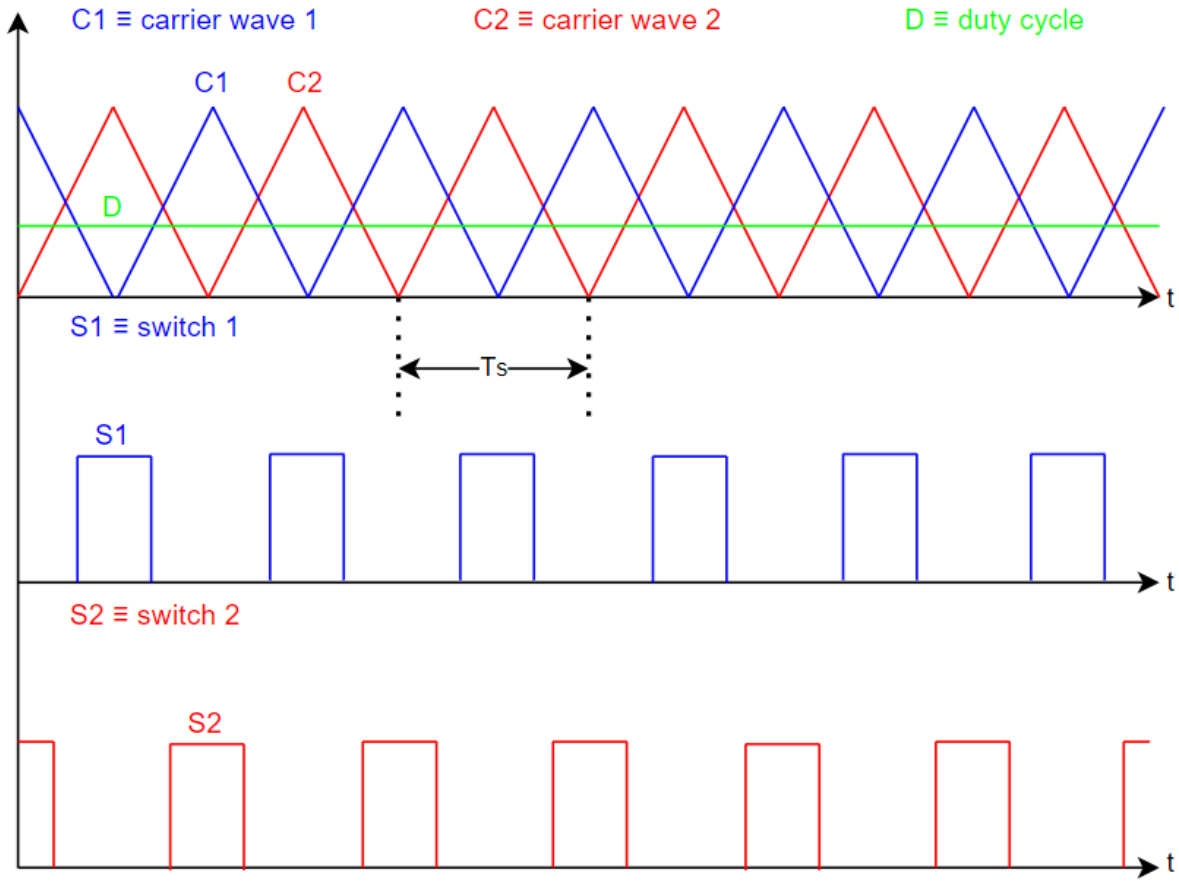

Figure 3: Commutation

As previously said, there are 4 switches working in a complementary manner, meaning that if there is S1 and $\overline{S1}$, $\overline{S1}$ instead of a switch, it will be a diode. Therefore, only S1 and S2 will be analysed.

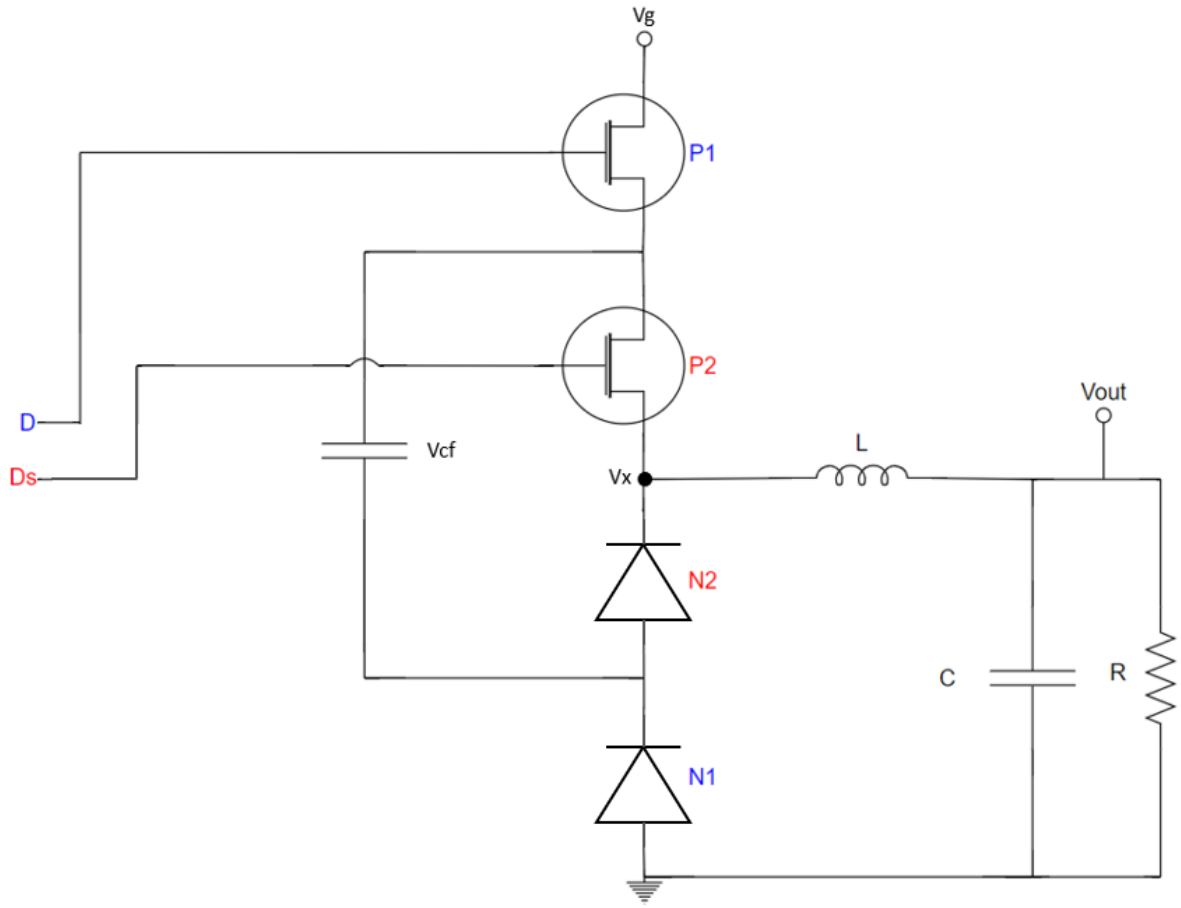

Figure 4: P1 complementary to N1 and P2 complementary to N2

The duty cycle being used must be taken in account since if the duty cycle is below or equal to 50%, then the duty cycle=D1 (Figure 5) and when duty cycle is above 50%, duty cycle=D1+0.5. This will only be true in the case where D1=D3 and D2=D4 (refer to Figure 5).

From now on, the switches N2 and N1 observed in Figure **4**, will be diodes as mentioned earlier.

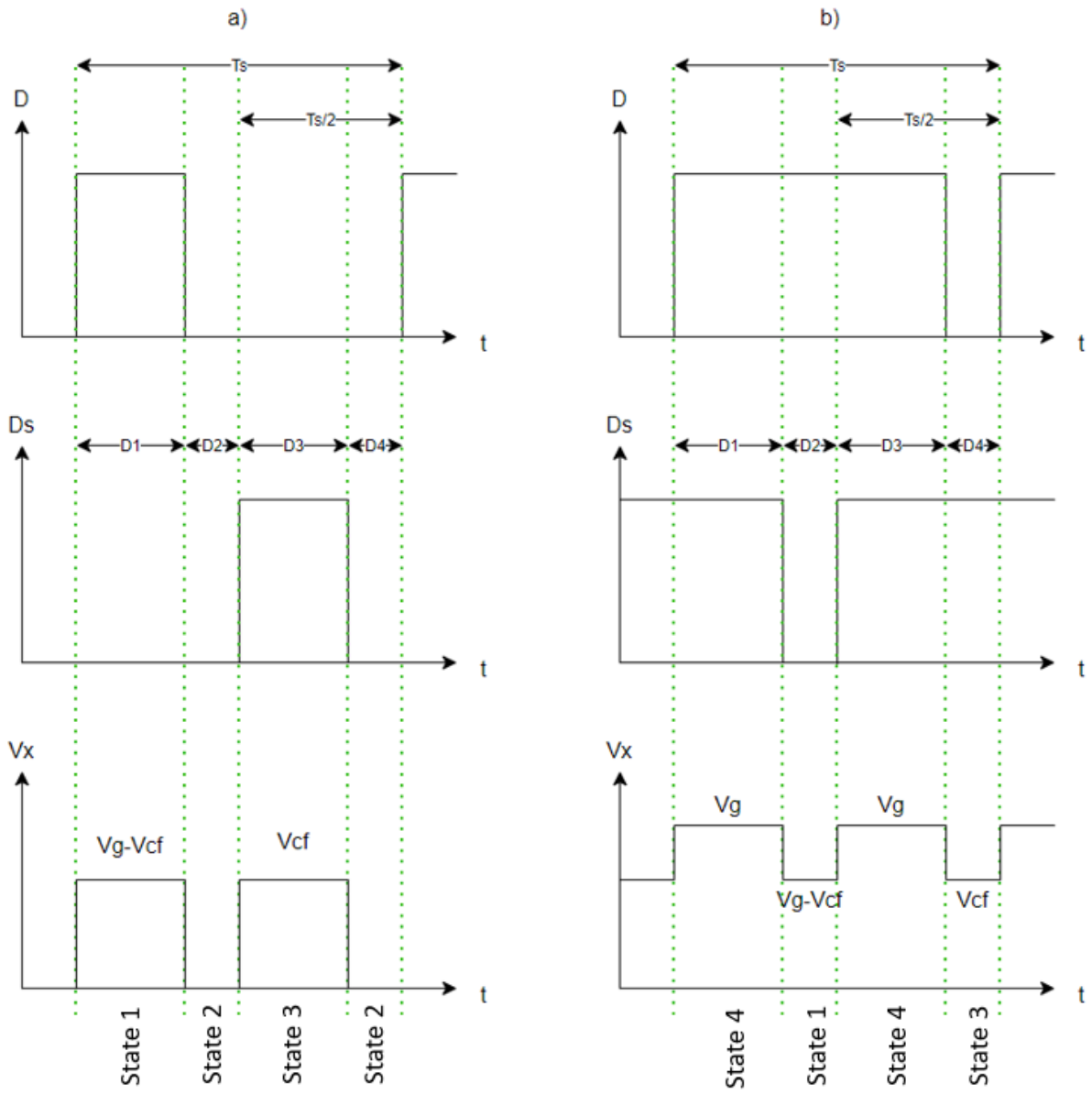

Figure 5: a) duty cycle ≤0.5 b) duty cycle>0.5 (Refer to Figure 4)

In order to have a clearer idea of the graph's shapes in Figure 5, refer to Figure 6.

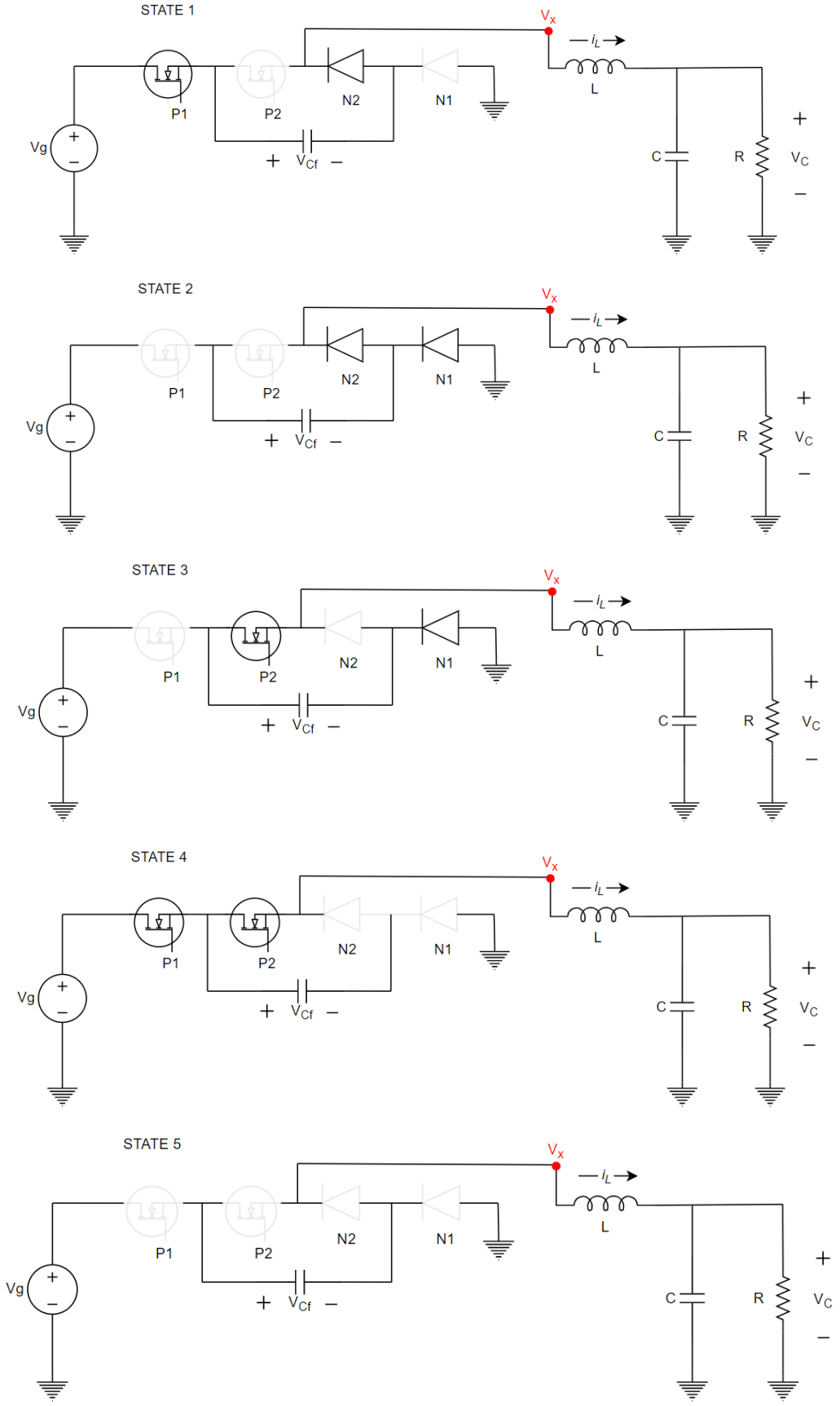

Figure 6: Possible working states of the converter

In Figure 6, the main purpose of the multilevel converter can be appreciated. In state 1, it can easily be seen how Vg charges the flying capacitor leaving:

$$V_X = \frac{1}{2}V_g \tag{3}$$

In state 3, the same thing happens since the flying capacitor is now the voltage source and again equation **(3)** takes place.

As previously mentioned, the analysis of this converter will be done by always assuming a duty cycle below 50%, meaning that the working state number 4 will be ignored.

2.2 Conduction modes

When studying the conduction modes, it needs to be taken in account the slope of $i_L(t)$ (inductor current). The voltage across de inductor (V_L) will have a serious effect on the slope.

$$V_L = L\frac{di_L}{dt} \rightarrow \frac{di_L}{dt} = \frac{V_L}{L} \tag{4}$$

V_L changes depending on the working state of the capacitor (Figure 6). When analysing the converter is being assumed that V_{CF} is stable and it's always half of V_g, the proof of this assumption is given in.

STATE 1:

$$V_L = V_X - V_O = (V_g - V_{CF}) - V_O \rightarrow \frac{di_L}{dt} = \frac{(V_g - V_{CF}) - V_O}{L} = \frac{\frac{V_g}{2} - V_O}{L} = \boldsymbol{\frac{V_g - 2V_O}{2L}} \tag{5}$$

STATE 2:

$$V_L = V_X - V_O = 0 - V_O \rightarrow \boldsymbol{\frac{di_L}{dt} = \frac{-V_O}{L}} \tag{6}$$

STATE 3:

$$V_L = V_X - V_O = V_{CF} - V_O \rightarrow \frac{di_L}{dt} = \frac{V_{CF} - V_O}{L} = \boldsymbol{\frac{V_g - 2V_O}{2L}} \tag{7}$$

STATE 4: Only occurring when the duty cycle is above 50% which isn't the case in this study.

$$V_L = V_X - V_O = V_g - V_O \rightarrow \frac{\boldsymbol{di_L}}{\boldsymbol{dt}} = \frac{\boldsymbol{V_g - V_O}}{\boldsymbol{L}} \quad \textbf{(8)}$$

STATE 5: Only occurring when working in DCM.

$$V_L = V_X - V_O = V_O - V_O = 0 \quad \textbf{(9)}$$

2.2.1 Continuous conduction mode (CCM)

This mode takes place when the inductor current never gets to fully discharge.

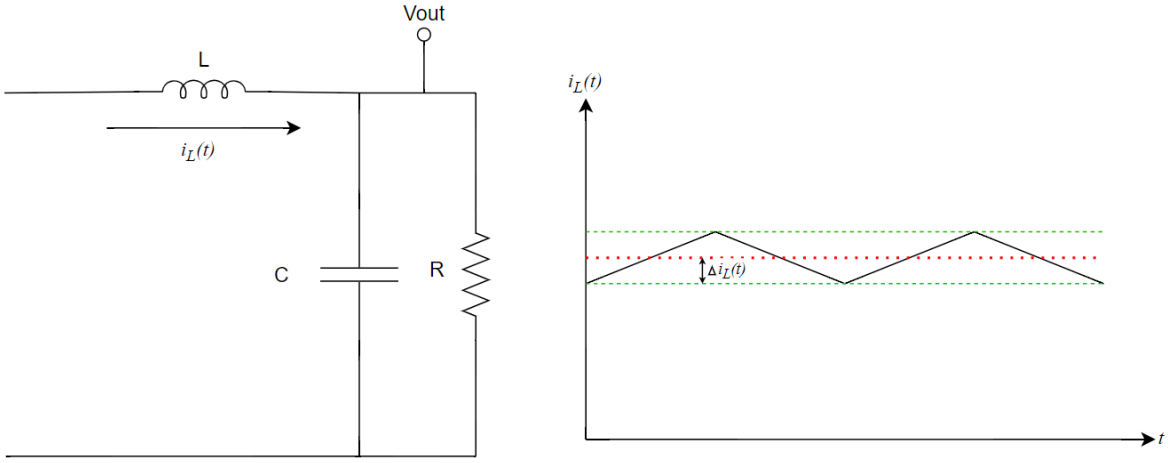

Figure 7: Inductor current in CCM

Studying the ripple of the inductor current is very important since is directly related to the slope that has been mentioned previously. The ripple can either be studied during the charging state or discharging state of the inductor. For this study the following will be considered.

$$\Delta i_L = \int_0^{t_1} V_L(t)dt \quad \textbf{(10)}$$

Where t_1 has different intervals. Referring back to Figure 3, leaves the following states (Figure 5 and Figure 6):

D1 → STATE 1

D2 → STATE 2

D3 → STATE 3

D4 → STATE 2

Finally, it can all be put together as shows:

$$\Delta i_L = \begin{cases} \dfrac{V_g(t) - 2V_O(t)}{2L} & for \quad t < T_S D \\ \dfrac{-V_O(t)}{L} & for \quad T_S D < t < \dfrac{T_S}{2} \\ \dfrac{V_g(t) - 2V_O(t)}{2L} & for \quad \dfrac{T_S}{2} < t < \dfrac{T_S}{2} + T_S D = \dfrac{T_S(1+2D)}{2} \\ \dfrac{-V_O(t)}{L} & for \quad \dfrac{T_S(1+2D)}{2} < t < T_S \end{cases} \qquad \textbf{(11)}$$

Going back to expression **(11)**, applying the small ripple approximation, assumes that $V_g(t) \approx V_g$ and $V_o(t) \approx V_o$, meaning that in order to find out the current ripple

These intervals may not be easy to understand straight forward, so analysing *Figure 3,* leaves *Figure 8* where it can easily be seen where these intervals come from.

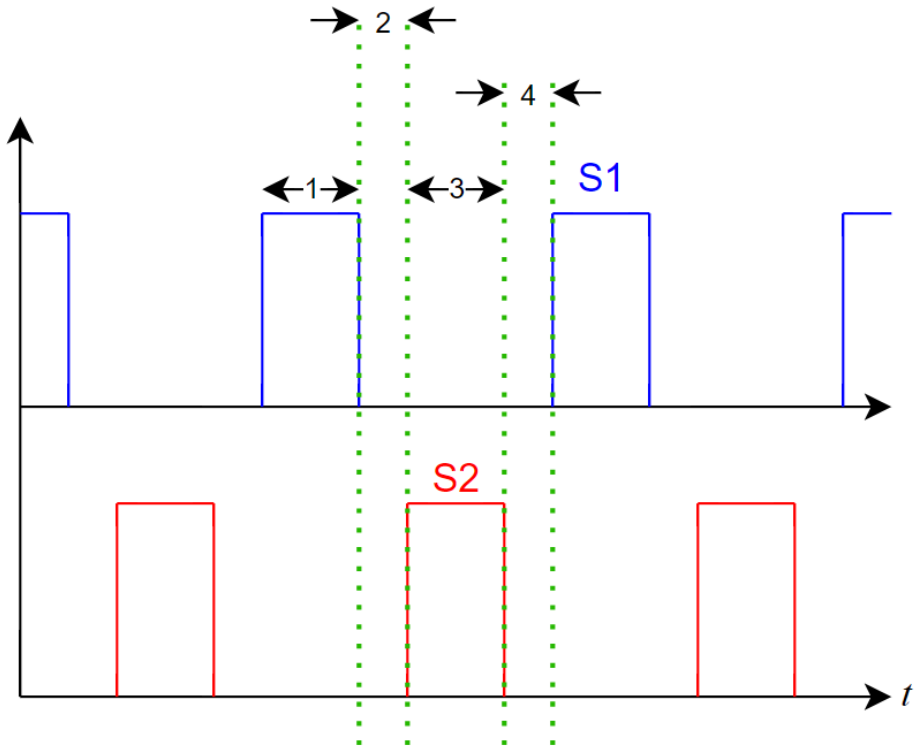

Figure 8: Analysis of the switches S1 and S2

The duty cycle is simply a proportion that refers to the period of time that the square wave is ON. The first interval is simply that proportion. The second interval goes up to $T_s/2$ as long as the duty cycle is always being kept below 50% and that the two carrier waves are always being phase shifted by 180º. The third interval follows the same criteria but starting halfway of the wave. Finally, the fourth interval is just arriving to the end of T_s.

For the converter to be in CCM it must be respected that $i_L > \Delta i_L$. As it can be seen in *Figure 7,* if $i_L < \Delta i_L$ then the inductor current would reach 0 A.

2.2.2 Discontinuous conduction mode (DCM)

This happens when the inductor current reaches 0 A, only in DCM the fifth state of the converter's possible states takes place.

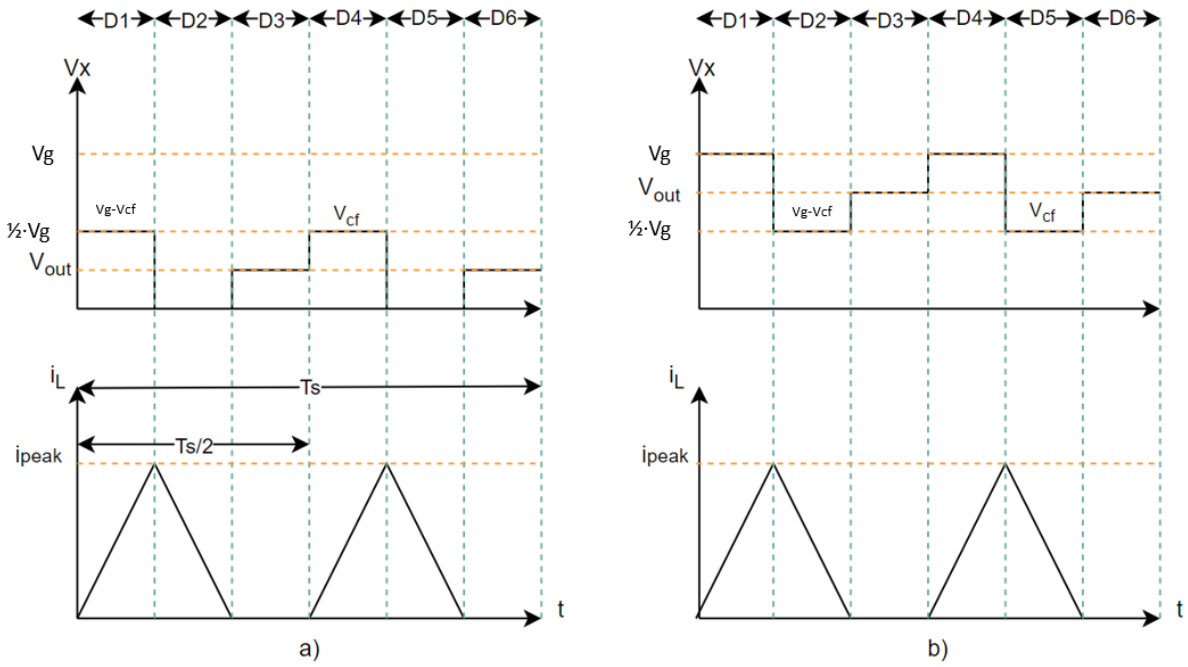

Figure 9: a) Duty cycle below or equal to 50% b) Duty cycle above 50%

In this conduction mode, the ripple still has a similar behaviour apart from the introduction of the fifth working state mentioned above. Therefore, the following rules:

D1 → STATE 1

D2 → STATE 2

D3 → STATE 5

D4 → STATE 3

D5 → STATE 2

D6 → STATE 5

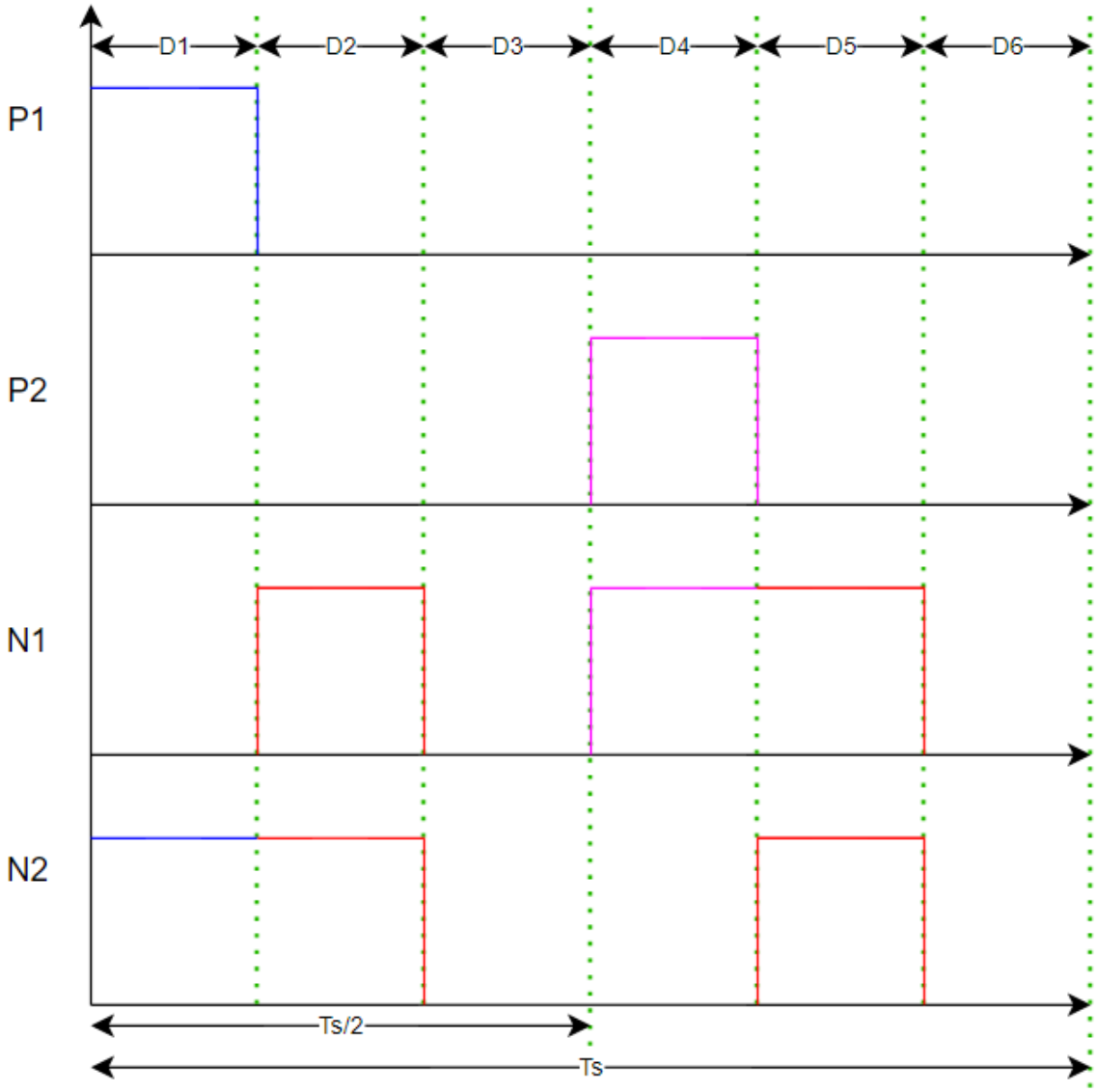

Figure 10: DCM commutation

2.3 Converter's output

When there's an input, the output has two parts, the transient part and the steady state part, where the steady state part is the equilibrium point and the transient part is the process in order to reach the steady state output. It must be clarified that when a perturbation is introduced there will also be a transient part. The converter's behaviour can be modelled in a way that a lineal averaged model is achieved, further it will be explained why this is mentioned.

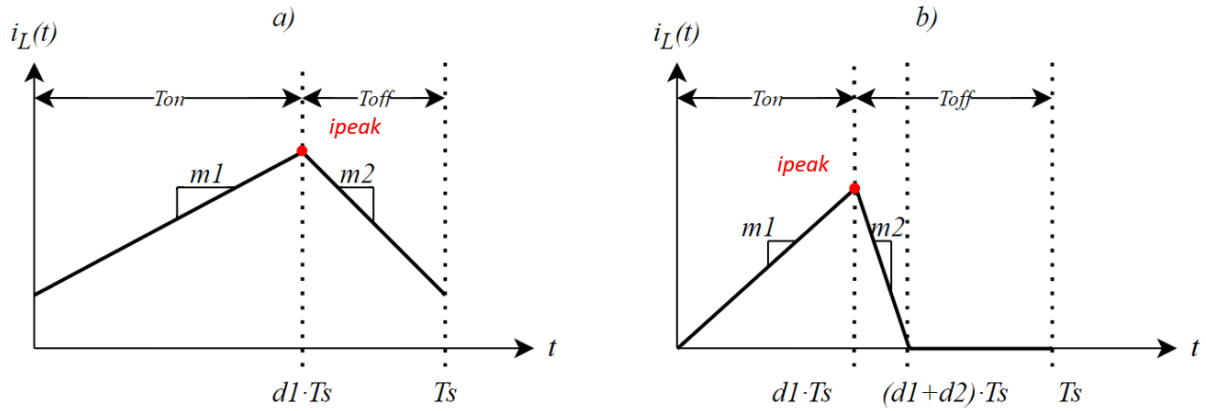

Figure 11: a) CCM and b) DCM

The goal of obtaining this model is so that the controller for the voltage-mode controller can be designed.

The converter is modelled by the following equations containing matrices:

ON (Period d_1T_S):

$$\begin{cases} \dfrac{dx(t)}{dt} = A_{ON}x(t) + B_{ON}\omega(t) \\ y(t) = C_{ON}x(t) + D_{ON}\omega(t) \end{cases} \quad \textbf{(12)}$$

OFF (Period d_2T_S):

$$\begin{cases} \dfrac{dx(t)}{dt} = A_{OFF}x(t) + B_{OFF}\omega(t) \\ y(t) = C_{OFF}x(t) + D_{OFF}\omega(t) \end{cases} \quad \textbf{(13)}$$

_ (Period $(1-d_1-d_2)T_S$):

$$\begin{cases} \dfrac{dx(t)}{dt} = A\_x(t) + B\_\omega(t) \\ y(t) = C\_x(t) + D\_\omega(t) \end{cases} \quad \textbf{(14)}$$

Where:

$$x(t) \equiv state\ variable \quad \omega(t) \equiv disturbance\ inputs \quad y(t) \equiv output$$

$$\boldsymbol{x(t)} = \begin{bmatrix} \boldsymbol{i_L(t)} \\ \\ \boldsymbol{V_C(t)} \end{bmatrix} \quad \boldsymbol{y} \quad \boldsymbol{\omega(t)} = \begin{bmatrix} \boldsymbol{V_g(t)} \\ \\ \boldsymbol{0} \end{bmatrix}$$

In order to obtain the matrices mentioned above, the converter's behaviour in each state (*Figure 6*) is analysed.

STATE 1

KVL (*Kirchhoff's Voltage Law*):

$$V_g(t) = V_{CF}(t) + L\frac{di_L}{dt} + V_C(t) \rightarrow V_g(t) = \frac{V_g(t)}{2} + L\frac{di_L}{dt} + V_C(t) \rightarrow \frac{V_g(t)}{2} = L\frac{di_L}{dt} + V_C(t)$$

$$\therefore \boldsymbol{\frac{di_L}{dt} = \frac{V_g(t)}{2L} - \frac{V_C(t)}{L}}$$

KCL (*Kirchhoff's Current Law*):

$$i_L(t) = i_C(t) + i_R(t) \rightarrow i_L(t) = C \cdot \frac{dV_C}{dt} + \frac{V_C(t)}{R}$$

$$\therefore \boldsymbol{\frac{dV_C}{dt} = \frac{i_L(t)}{C} - \frac{V_C(t)}{RC}}$$

STATE 2

KVL:

$$L \cdot \frac{di_L}{dt} = -V_C(t)$$

$$\therefore \boldsymbol{\frac{di_L}{dt} = -\frac{V_C(t)}{L}}$$

KCL:

$$i_L(t) = i_C(t) + i_R(t) \rightarrow i_L(t) = C\frac{dV_C}{dt} + \frac{V_C(t)}{R}$$

$$\therefore \boldsymbol{\frac{dV_C}{dt} = \frac{i_L(t)}{C} - \frac{V_C(t)}{RC}}$$

STATE 3

KVL:

$$V_{CF}(t) = L\frac{di_L}{dt} + V_C(t) \rightarrow \frac{V_g(t)}{2} = L\frac{di_L}{dt} + V_C(t) \rightarrow \frac{V_g(t)}{2} = L\frac{di_L}{dt} + V_C(t)$$

$$\therefore \boldsymbol{\frac{di_L}{dt} = \frac{V_g(t)}{2L} - \frac{V_C(t)}{L}}$$

KCL:

$$i_L(t) = i_C(t) + i_R(t) \rightarrow \ i_L(t) = C\frac{dV_C}{dt} + \frac{V_C(t)}{R}$$

$$\therefore \ \boldsymbol{\frac{dV_C}{dt} = \frac{i_L(t)}{C} - \frac{V_C(t)}{RC}}$$

STATE 5

KVL:

$$i_L(t) = 0$$

$$\therefore \ \boldsymbol{\frac{di_L}{dt} = 0}$$

KCL:

$$i_C(t) = -i_R(t) \rightarrow \ C\frac{dV_C}{dt} = -\frac{V_C(t)}{R}$$

$$\therefore \ \boldsymbol{\frac{dV_C}{dt} = -\frac{V_C(t)}{RC}}$$

It can be seen how the first and third state end up being the same, building up on these states A_{ON} and B_{ON} are obtained, for the second state A_{OFF} and B_{OFF} are obtained, finally from the fifth state A_ and B_ are obtained.

$$\boldsymbol{A_{ON} = \begin{bmatrix} 0 & -\frac{1}{L} \\ \frac{1}{C} & -\frac{1}{RC} \end{bmatrix} \qquad B_{ON} = \begin{bmatrix} \frac{1}{2L} \\ 0 \end{bmatrix}} \qquad \textbf{(15)}$$

$$\boldsymbol{A_{OFF} = \begin{bmatrix} 0 & -\frac{1}{L} \\ \frac{1}{C} & -\frac{1}{RC} \end{bmatrix} \qquad B_{OFF} = \begin{bmatrix} 0 \\ 0 \end{bmatrix}} \qquad \textbf{(16)}$$

$$\boldsymbol{A\_} = \begin{bmatrix} \mathbf{0} & \mathbf{0} \\ \mathbf{0} & -\dfrac{\mathbf{1}}{\boldsymbol{RC}} \end{bmatrix} \qquad \boldsymbol{B\_} = \begin{bmatrix} \mathbf{0} \\ \mathbf{0} \end{bmatrix} \tag{17}$$

In CCM the following rules the converter's behaviour:

$$\begin{cases} \dfrac{d\bar{x}}{dt} = \left(\overline{d1}(t)A_{ON} + (1-\overline{d1}(t))A_{OFF}\right)\bar{x}(t) + \left(\overline{d1}(t)B_{ON} + \left(1-\overline{d1}(t)\right)B_{OFF}\right)\bar{\omega}(t) \\ \bar{y}(t) = \left(\overline{d1}(t)C_{ON} + (1-\overline{d1}(t))C_{OFF}\right)\bar{x}(t) + \left(\overline{d1}(t)D_{ON} + \left(1-\overline{d1}(t)\right)D_{OFF}\right)\bar{\omega}(t) \end{cases} \tag{18}$$

Where:

$$\bar{x}(t) \equiv Averaged\ state\ variable$$

$$\bar{y}(t) \equiv Averaged\ output$$

$$\bar{x}(t) = X + \hat{x}(t)$$

$$\bar{\omega}(t) = W + \hat{\omega}(t)$$

$$\overline{d1}(t) = \bar{u}(t) = U + \hat{u}(t)$$

$$\bar{y}(t) = Y + \hat{y}(t)$$

Where *X, W, U* and *Y* are the steady state values and $\hat{x}, \hat{\omega}, \hat{u}$ and $\hat{y}$ are the incremental part of the variable.

However as previously clarified, in this final project the main focus is to analyse the converter's behaviour in DCM, this means taking in account the expression (*18)* with a slightly difference (*Figure 10*):

$$\begin{cases} \dfrac{d\bar{x}}{dt} = \left(\overline{d1}(t)A_{ON} + \overline{d2}(t)A_{OFF} + \left(1-\overline{d1}(t)-\overline{d2}(t)\right)A\_\right)M\bar{x}(t) + \left(\overline{d1}(t)B_{ON} + \overline{d2}(t)B_{OFF} + \left(1-\overline{d1}(t)-\overline{d2}(t)\right)B\_\right)M\bar{\omega}(t) \\ \bar{y}(t) = \left(\overline{d1}(t)C_{ON} + \overline{d2}(t)C_{OFF} + \left(1-\overline{d1}(t)-\overline{d2}(t)\right)C\_\right)M\bar{x}(t) + \left(\overline{d1}(t)D_{ON} + \overline{d2}(t)D_{OFF} + \left(1-\overline{d1}(t)-\overline{d2}(t)\right)D\_\right)M\bar{\omega}(t) \end{cases} \tag{19}$$

In this case the matrix M is:

$$\boldsymbol{M} = \begin{bmatrix} \dfrac{\mathbf{1}}{\overline{\boldsymbol{d1}}(\boldsymbol{t}) + \overline{\boldsymbol{d2}}(\boldsymbol{t})} & \mathbf{0} \\ \mathbf{0} & \mathbf{1} \end{bmatrix} \tag{20}$$

Using the expressions *(19)* and *(20)*, the following is obtained:

$$\begin{bmatrix} \frac{d\bar{\imath}_L}{dt} \\ \frac{d\bar{v}_C}{dt} \end{bmatrix} = \left(\begin{bmatrix} 0 & -\frac{\overline{d1}(t)}{L} \\ \frac{\overline{d1}(t)}{C} & -\frac{\overline{d1}(t)}{RC} \end{bmatrix} + \begin{bmatrix} 0 & -\frac{\overline{d2}(t)}{L} \\ \frac{\overline{d2}(t)}{C} & -\frac{\overline{d2}(t)}{RC} \end{bmatrix} + \begin{bmatrix} 0 & 0 \\ 0 & -\frac{(1-\overline{d1}(t)-\overline{d2}(t))}{RC} \end{bmatrix} \right) \begin{bmatrix} \frac{1}{\overline{d1}(t)+\overline{d2}(t)} & 0 \\ 0 & 1 \end{bmatrix} \begin{bmatrix} \bar{\imath}_L(t) \\ \bar{v}_C(t) \end{bmatrix} + \begin{bmatrix} \frac{\overline{d1}(t)}{2L} \\ 0 \end{bmatrix} \begin{bmatrix} \bar{v}_g(t) \\ 0 \end{bmatrix}$$

$$\begin{bmatrix} \frac{d\bar{\imath}_L}{dt} \\ \frac{d\bar{v}_C}{dt} \end{bmatrix} = \begin{bmatrix} 0 & \frac{-\overline{d1}(t)-\overline{d2}(t)}{L} \\ \frac{\overline{d1}(t)+\overline{d2}(t)}{C} & -\frac{1}{RC} \end{bmatrix} \begin{bmatrix} \frac{1}{\overline{d1}(t)+\overline{d2}(t)} & 0 \\ 0 & 1 \end{bmatrix} \begin{bmatrix} \bar{\imath}_L(t) \\ \bar{v}_C(t) \end{bmatrix} + \begin{bmatrix} \frac{\overline{d1}(t)}{2L} \\ 0 \end{bmatrix} \begin{bmatrix} \bar{v}_g(t) \\ 0 \end{bmatrix}$$

$$\begin{bmatrix} \frac{d\bar{\imath}_L}{dt} \\ \frac{d\bar{v}_C}{dt} \end{bmatrix} = \begin{bmatrix} 0 & \frac{-\overline{d1}(t)-\overline{d2}(t)}{L} \\ \frac{1}{C} & -\frac{1}{RC} \end{bmatrix} \begin{bmatrix} \bar{\imath}_L(t) \\ \bar{v}_C(t) \end{bmatrix} + \begin{bmatrix} \frac{\overline{d1}(t)\bar{v}_g(t)}{2L} \\ 0 \end{bmatrix}$$

$$\begin{cases} \boldsymbol{\frac{d\bar{\imath}_L}{dt} = -\frac{\overline{d1}(t)+\overline{d2}(t)}{L}\bar{v}_C(t) + \frac{\overline{d1}(t)}{2L}\bar{v}_g(t)} \\ \boldsymbol{\frac{d\bar{v}_C}{dt} = \frac{1}{C}\bar{\imath}_L(t) - \frac{1}{RC}\bar{v}_C(t)} \end{cases} \quad \textbf{(20)}$$

Now, to have an expression that is no dependent on $\overline{d2}$, another expression in terms of $\overline{d1}$ can be substituted in [7]:

Peak current:

$$i_{pico} = m_1 \overline{d1}(t) T_s$$

Where:

$$m_1 = M1 + \widehat{m1}(t)$$

Inductor's averaged current:

$$\bar{\imath}_L(t) = \frac{m1\overline{d1}(t)T_s\left(\overline{d1}(t)+\overline{d2}(t)\right)}{2} \quad \textbf{(21)}$$

Rearranging *(21)* the following is obtained:

$$\overline{d2}(t) = \frac{2\bar{\imath}_L(t)}{m1\overline{d1}(t)T_s} - \overline{d1}(t) \quad \textbf{(22)}$$

$$\begin{cases} \dfrac{d\bar{\imath}_L}{dt} = -\dfrac{\overline{d1}(t) + \dfrac{2\bar{\imath}_L(t)}{m1\overline{d1}(t)T_s} - \overline{d1}(t)}{L}\bar{v}_C + \dfrac{\overline{d1}(t)\bar{v}_g(t)}{2L} = -\dfrac{\dfrac{2\bar{\imath}_L(t)}{m1\overline{d1}(t)T_s}}{L}\bar{v}_C + \dfrac{\overline{d1}(t)}{2} \\ \dfrac{d\bar{v}_C}{dt} = \dfrac{1}{C}\bar{\imath}_L(t) - \dfrac{1}{RC}\bar{v}_C(t) \end{cases} \quad \textbf{(23)}$$

2.3.1 Matrix M

In DCM the following is known:

$$\dot{x}(t) = A_1 x(t) + B_1 v_{in}(t) \qquad t \in [0, d1 \cdot T]$$

$$\dot{x}(t) = A_2 x(t) + B_2 v_{in}(t) \qquad t \in [\, d1 \cdot T, ((d1 + d2) \cdot T)]$$

$$\dot{x}(t) = A_3 x(t) + B_3 v_{in}(t) \qquad t \in [((d1 + d2) \cdot T), T$$

As seen in CCM, the following model would be given:

$$\dot{\bar{x}} = (d1A_1 + d2A_2 + (1 - d1 - d2)A_3)\bar{x} + (d1B_1 + d2B_2 + (1 - d1 - d2)B_3)v_{in}$$

The problem with this averaging method in DCM, is that only the values of the matrices are averaged, and the state variables are no considered.

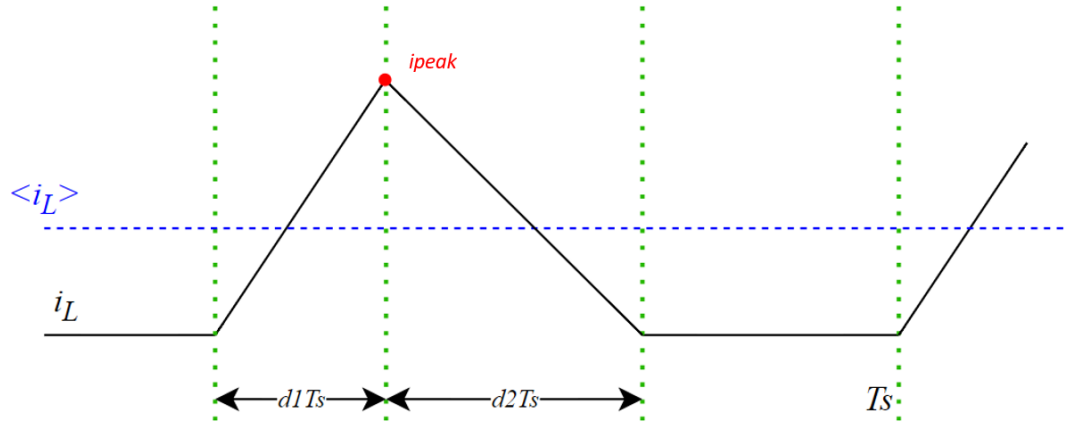

Figure 12: Inductor current in DCM

Referring to *Figure 13 (<i_L> = $\bar{\imath}_L$)*, an averaged inductor current can be obtained as it shows in the following:

$$\bar{\imath}_L = \frac{d1 i_{peak}}{2} + \frac{d2 i_{peak}}{2} = \frac{i_{peak}}{2}(d1 + d2) \qquad \textbf{(24)}$$

Is basically the same expression as in CCM, only that now *d2* appears. To easily understand this analysis, consider that in the ON interval, where the flying capacitor is connected to the inductor, in other words $t \in [0, d1 \cdot Ts]$, the current that receives the

capacitor is not the same as the average current of the inductor. It's convenient to formulate this behaviour in terms of the capacitor's charge and discharge state.

$$Q_C = I_C \cdot \Delta t = \frac{i_{peak}}{2} d1 T_s \quad \textbf{(25)}$$

Now from the expression *(22)*:

$$I_C = \frac{Q_C}{\Delta t} = \frac{Q_C}{T_s} = \frac{i_{peak} d1}{2} \quad \textbf{(26)}$$

Now considering the resistive load, using *KCL*, the following is obtained:

$$C \cdot \frac{dv_C}{dt} = \frac{i_{peak} d1}{2} - \frac{v_C}{R} \quad \textbf{(27)}$$

Going back to what was said previously, if CCM like averaging was done, the current received by the capacitor would have been $\bar{\imath}_L \cdot d1$, which would be the state-spaced averaged (SSA)

$$I_C = \bar{\imath}_L \cdot d1 = \frac{i_{peak} \cdot d1}{2} \cdot (d1 + d2) \qquad (SSA\ capacitor\ current)$$

$$I_C = \frac{i_{peak} \cdot d1}{2} \qquad (real\ capacitor\ current)$$

By applying the same concept as in the ON analysis, it can be done for the OFF state so an averaged model can be obtained.

Table 1: Capacitor's current comparison

Inductor charging the capacitor	Capacitor's current (SSA)	Capacitor's current (real)
ON	$\bar{\imath}_L d1 = \frac{i_{peak} d1}{2}(d1 + d2)$	$I_C = \frac{i_{peak} d1}{2}$
OFF	$\bar{\imath}_L d2 = \frac{i_{peak} d2}{2}(d1 + d2)$	$I_C = \frac{i_{peak} d2}{2}$
Whole cycle	$\bar{\imath}_L (d1 + d2) = \frac{i_{peak}}{2}(d1 + d2)^2$	$I_C = \frac{i_{peak}}{2}(d1 + d2)$

Looking at *Table 1*, we can see the difference between the *SSA* and the real current, this can be fixed by applying the following:

$$\boldsymbol{M = diag\left[\frac{1}{d1 + d2}, \dots, \frac{1}{d1 + d2}, 1, \dots, 1\right] = \begin{bmatrix} \frac{1}{d1 + d2} & \dots & 0 \\ \vdots & \ddots & \vdots \\ 0 & \dots & 1 \end{bmatrix}} \quad \textbf{(28)}$$

The amount of $\frac{1}{d1+d2}$ terms appearing in the matrix is related to the amount of state variables in DCM.

2.3.2 Steady state model

Referring to the expression (23) and knowing that a steady state model is the goal, the derivatives are set equal to 0 and the incremental values are considered negligible and only steady state variables are used.

$$\begin{cases} 0 = -\frac{2I_L}{M1UT_sL} V_C + \frac{UV_g}{2L} \\ 0 = \frac{1}{C} I_L - \frac{1}{RC} V_C \end{cases} \quad \textbf{(29)}$$

Looking back to expression *(5)*:

$$m1 = \frac{\frac{V_g}{2} - V_O}{L} = \frac{\frac{V_g}{2} - V_C}{L}$$

Therefore:

$$\begin{cases} \mathbf{0} = -\dfrac{\mathbf{2I_L}}{\left(\dfrac{\mathbf{V_g}}{\mathbf{2}} - \mathbf{V_C}\right)\mathbf{UT_s}}\mathbf{V_C} + \dfrac{\mathbf{UV_g}}{\mathbf{2L}} \\ \mathbf{0} = \dfrac{\mathbf{I_L}}{\mathbf{C}} - \dfrac{\mathbf{V_C}}{\mathbf{RC}} \quad \rightarrow \quad \mathbf{I_L} = \dfrac{\mathbf{V_C}}{\mathbf{R}} \end{cases} \tag{30}$$

Expression *(30)* can be rearranged into one single equation to end up having a steady state output voltage expression:

$$-\frac{2\left(\frac{V_C}{R}\right)V_C}{\left(\frac{V_g}{2} - V_C\right)UT_s} + \frac{UV_g}{2L} = 0 \tag{31}$$

(31) can also be further rearranged to end up having a standard quadratic expression:

$$-4\left(\frac{V_C}{R}\right)V_C L + U^2 V_g T_s \left(\frac{V_g}{2} - V_C\right) = -4\frac{L}{R}V_C^2 - U^2 V_g T_s V_C + \frac{V_g^2}{2}U^2 T_s = 0 \tag{32}$$

It can be seen how *(32)* is a quadratic expression:

$$x^2 + bx + c = 0$$

Where:

$$a = -\frac{4L}{R} \qquad b = -U^2 V_g T_s \qquad c = \frac{V_g^2}{2}U^2 T_s$$

Therefore, knowing that the output voltage is V_C:

$$V_C = \frac{-b \pm \sqrt{b^2 - 4ac}}{2a}$$

$$V_{C1} = \frac{U^2 V_g T_s + \sqrt{U^4 V_g^2 {T_s}^2 + 4 \cdot \frac{4L}{R} \cdot \frac{V_g^2}{2}U^2 T_s}}{-2 \cdot \frac{4L}{R}}$$

$$V_{C2} = \frac{U^2 V_g T_s - \sqrt{U^4 V_g^2 {T_s}^2 + 4 \cdot \frac{4L}{R} \cdot \frac{V_g^2}{2}U^2 T_s}}{-2 \cdot \frac{4L}{R}}$$

As it can be seen, V_{C1} will always be negative which is impossible in a Buck converter, therefore the right option is V_{C2}.

$$V_O = \frac{U^2 V_g T_s - \sqrt{U^4 V_g^2 {T_s}^2 + 4 \cdot \frac{4L}{R} \cdot \frac{V_g^2}{2} U^2 T_s}}{-2 \cdot \frac{4L}{R}} \quad \textbf{(33)}$$

2.3.3 Dynamic model

The goal is to obtain a model in the format of ẋ=Ax+Bω, which is a lineal model, the problem when it comes to do the dynamic model, is that the expression (23) is not lineal since there are a few time dependant variables multiplying each other, leaving t2 terms. To solve this problem the system needs to be linearized (Jacobian). It must be clarified that the main purpose of this model is to consider the incremental parts of the variables in the model.

$$\begin{cases} \frac{dI_L}{dt} + \frac{d\hat{\imath}_L}{dt} = f_{\bar{\imath}_L}(I_L, V_C, V_g, U) + \hat{\imath}_L \frac{\partial f_{\bar{\imath}_L}(\bar{\imath}_L, V_C, V_g, U)}{\partial \hat{\imath}_L}\Big|_{\bar{\imath}_L = I_L} + \hat{v}_c \frac{\partial f_{\bar{\imath}_L}(I_L, \bar{v}_C, V_g, U)}{\partial \hat{v}_C}\Big|_{\bar{v}_C = V_C} + \hat{d}_1 \frac{\partial f_{\bar{\imath}_L}(I_L, V_C, V_g, \bar{d}_1)}{\partial \hat{d}_1}\Big| \\ \frac{dV_L}{dt} + \frac{d\hat{v}_L}{dt} = f_{\bar{v}_C}(I_L, V_C, V_g) + \hat{\imath}_L \frac{\partial f_{\bar{\imath}_L}(\bar{\imath}_L, V_C, V_g)}{\partial \hat{\imath}_L}\Big|_{\bar{\imath}_L = I_L} + \hat{v}_c \frac{\partial f_{\bar{\imath}_L}(I_L, \bar{v}_C, V_g)}{\partial \hat{v}_C}\Big|_{\bar{v}_C = V_C} \end{cases} \quad \textbf{(34)}$$

$$\frac{\partial f_{\bar{\imath}_L}(\bar{\imath}_L, V_C, V_g, U)}{\partial \hat{\imath}_L}\Big|_{\bar{\imath}_L = I_L} = \frac{\partial f_{\bar{\imath}_L}\left(-\frac{2\bar{\imath}_L(t)}{\left(\frac{V_g}{2} - V_C\right)UT} V_C + \frac{U}{2L} V_g\right)}{\partial \hat{\imath}_L}\Bigg|_{\bar{\imath}_L = I_L} = -\frac{2V_C}{\left(\frac{V_g}{2} - V_C\right)UT}$$

$$\frac{\partial f_{\bar{\imath}_L}(I_L, \bar{v}_C, V_g, U)}{\partial \hat{v}_C}\Big|_{\bar{v}_C = V_C} = \frac{\partial f_{\bar{\imath}_L}\left(-\frac{2\frac{V_C}{R}}{\left(\frac{V_g}{2} - V_C\right)UT} \bar{v}_C + \frac{d1}{2L} V_g\right)}{\partial \hat{v}_C}\Bigg|_{\bar{v}_C = V_C} = -\frac{2\frac{V_C}{R} V_g}{\left(\frac{V_g}{2} - V_C\right)^2 UT}$$

$$\left.\frac{\partial f_{\bar{\imath}_L}(I_L,V_C,V_g,\bar{d}_1)}{\partial \hat{d}_1}\right|_{\bar{d}_1=U} = \left.\frac{\partial f_{\bar{\imath}_L}\left(-\frac{2\frac{V_C}{R}}{\left(\frac{V_g}{2}-V_C\right)\bar{d}_1 T}V_C+\frac{d1}{2L}V_g\right)}{\partial \hat{d}_1}\right|_{\bar{d}_1=U}$$

$$= \frac{2\frac{V_C^2}{R}}{\left(\frac{V_g}{2}-V_C\right)U^2T}\hat{d}_1+\frac{V_g}{2L}$$

$$\left.\frac{\partial f_{\bar{\imath}_L}(\bar{\imath}_L,V_C,V_g)}{\partial \hat{\imath}_L}\right|_{\bar{\imath}_L=I_L} = \left.\frac{\partial f_{\bar{\imath}_L}\left(\frac{1}{C}\bar{\imath}_L-\frac{1}{RC}V_C\right)}{\partial \hat{\imath}_L}\right|_{\bar{\imath}_L=I_L} = \frac{1}{C}$$

$$\left.\frac{\partial f_{\bar{\imath}_L}(I_L,\bar{v}_C,V_g)}{\partial \hat{v}_C}\right|_{\bar{v}_C=V_C} = \left.\frac{\partial f_{\bar{\imath}_L}\left(\frac{1}{C}I_L-\frac{1}{RC}\bar{v}_C\right)}{\partial \hat{v}_C}\right|_{\bar{v}_C=V_C} = -\frac{1}{RC}$$

Finally, everything is put in the following format:

$$\begin{cases}\frac{dI_L}{dt}+\frac{d\hat{\imath}_L}{dt} = -\frac{2I_L}{(V_g-V_C)UT}V_C+\frac{U}{2L}V_g-\frac{2V_C}{(V_g-V_C)UT}\hat{\imath}_L(t)-\frac{2\frac{V_C}{R}V_g}{(V_g-V_C)^2UT}\hat{v}_c(t)+\left(\frac{2\frac{V_C^2}{R}}{(V_g-V_C)U^2T}\hat{d}_1(t)+\frac{V_g}{2L}\right)\hat{d}_1(t)\\ \frac{dV_C}{dt}+\frac{d\hat{v}_C}{dt} = \frac{I_L}{C}-\frac{V_C}{RC}+\frac{1}{C}\hat{\imath}_L(t)-\frac{1}{RC}\hat{v}_c(t)\end{cases} \quad \textbf{(35)}$$

As said above, for the dynamic model the part that is important is the one including the incremental part of the variables:

The term including $\hat{d}_1(t)^2$ is neglected since is very small.

$$\begin{cases}\frac{d\hat{\imath}_L}{dt} = -\frac{2V_C}{(V_g-V_C)UT}\hat{\imath}_L(t)-\frac{2\frac{V_C}{R}V_g}{(V_g-V_C)^2UT}\hat{v}_c(t)+\frac{V_g}{2L}\hat{d}_1(t)\\ \frac{d\hat{v}_C}{dt} = \frac{1}{C}\hat{\imath}_L(t)-\frac{1}{RC}\hat{v}_c(t)\end{cases} \quad \textbf{(36)}$$

(36) can now be expressed in the form of *$\dot{x}$=Ax+Bω:*

$$\begin{bmatrix} \frac{d\hat{\imath}_L}{dt} \\ \\ \frac{d\hat{v}_C}{dt} \end{bmatrix} = \begin{bmatrix} -\frac{2V_C}{(V_g - V_C)UT} & -\frac{2\frac{V_C}{R}V_g}{(V_g - V_C)^2 UT} \\ \\ \frac{1}{C} & -\frac{1}{RC} \end{bmatrix} \begin{bmatrix} \hat{\imath}_L(t) \\ \\ \hat{v}_C(t) \end{bmatrix} + \begin{bmatrix} \frac{V_g}{2L} \\ \\ 0 \end{bmatrix} \hat{d}_1(t)$$

$$[\hat{v}_O(t)] = [0 \quad 1] \begin{bmatrix} \hat{\imath}_L(t) \\ \\ \hat{v}_C(t) \end{bmatrix}$$

In order to obtain the transfer function that describes de behaviour of the output voltage depending on the duty cycle, Laplace transform is needed to be applied:

$$\dot{\hat{x}}(t) = A\hat{x}(t) + B\hat{d}_1(t)$$

$$\hat{y}(t) = C\hat{x}(t)$$

$\mathcal{L}$:

$$s\hat{x}(s) = A\hat{x}(s) + B\hat{d}_1(s)$$

$$\hat{y}(s) = C\hat{x}(s)$$

Which leaves:

$$\frac{\hat{y}(s)}{\hat{d}_1(s)} = C((sI - A)^{-1} \cdot B)$$

Where:

$$A = \begin{bmatrix} -\frac{2V_C}{(V_g - V_C)UT} & -\frac{2\frac{V_C}{R}V_g}{(V_g - V_C)^2 UT} \\ \\ \frac{1}{C} & -\frac{1}{RC} \end{bmatrix}$$

$$B = \begin{bmatrix} \frac{V_g}{2L} \\ \\ 0 \end{bmatrix} \qquad C = [0 \quad 1]$$

Which ends up giving the following expression:

$$\frac{\hat{y}(s)}{\hat{d}_1(s)} = [0 \quad 1] \begin{bmatrix} -\frac{sUT(V_g - V_C) + 2V_C}{(V_g - V_C)UT} & -\frac{2\frac{V_C}{R}V_g}{(V_g - V_C)^2 UT} \\ \\ -\frac{1}{C} & -\frac{sRC + 1}{RC} \end{bmatrix}^{-1} \begin{bmatrix} \frac{V_g}{2L} \\ \\ 0 \end{bmatrix} \quad \textbf{(37)}$$

(37) can be re-written giving the simplified expression:

$$\frac{\hat{y}(s)}{\hat{d}_1(s)} = \frac{UTRV_g(V_g - V_C)^2 s}{2L(UTRV_C^2 s^2 C + UTV_C^2 s - 2RV_C^2 sC - 2V_C^2 + 2RV_g V_C sC + 4V_g V_C - 2UTRV_g V_C s^2 C - 2UTV_g V_C s + UTRV_g^2 V_C^2 s^2 C + UTV_g^2 s)} \quad \textbf{(38)}$$

3. Simulation

Once the steady state model and the dynamic model are obtained, they must be verified, to do this PSIM and MATLAB have been used.

3.1 Steady state model simulation

To verify this model, the power stage has been simulated in PSIM, the result from PSIM and the result obtained from expression (33) have been compared.

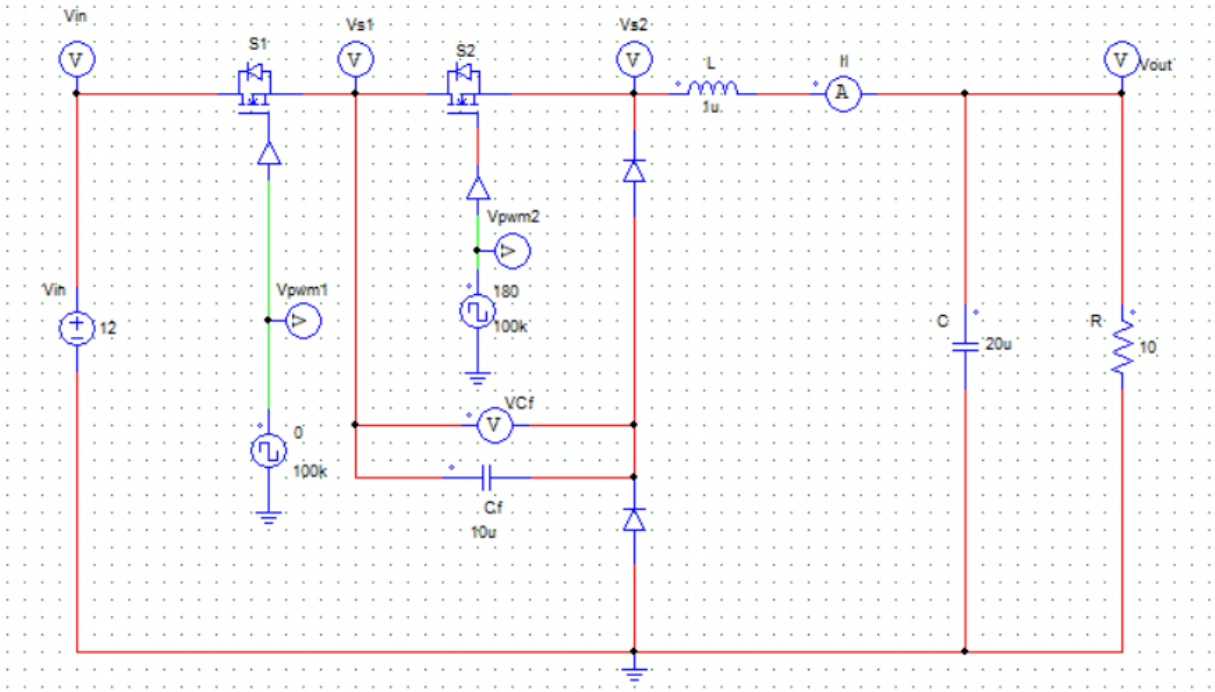

Figure 13: Circuit used to simulate the power stage

It's important to verify that in the simulation the switches commutation is adequate and that the converter is indeed working in DCM.

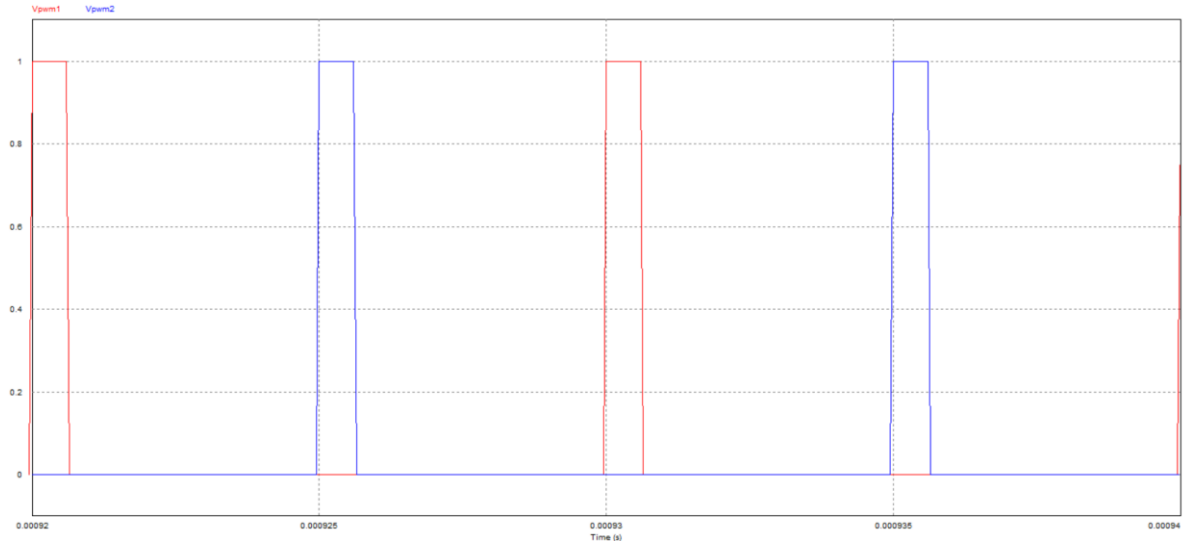

Figure 14: PWM signals that make the MOSFET switch (phase-shifted 180º)

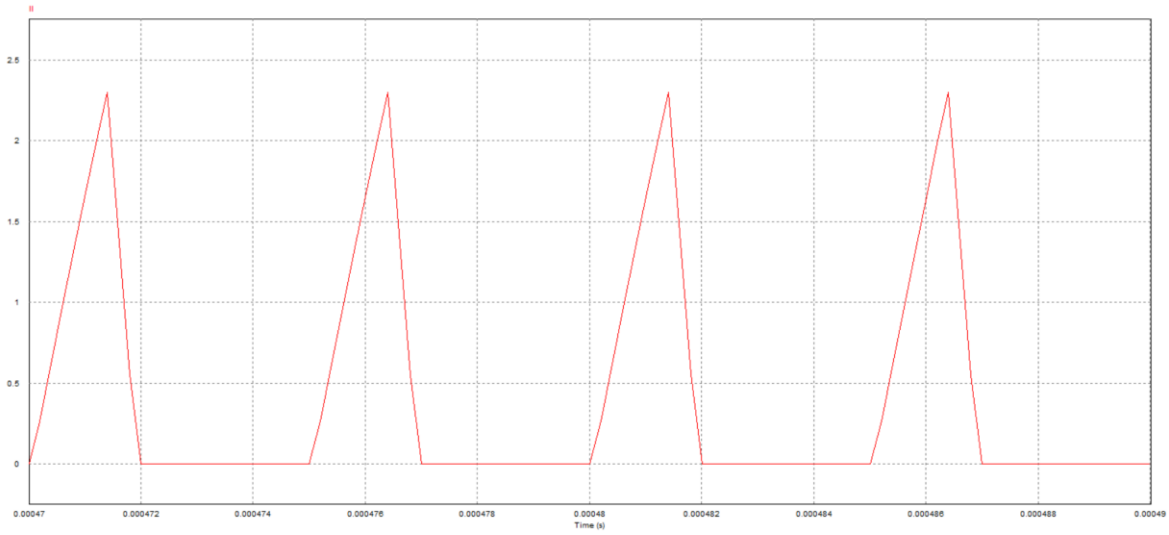

Figure 15: Inductor corrent (DCM)

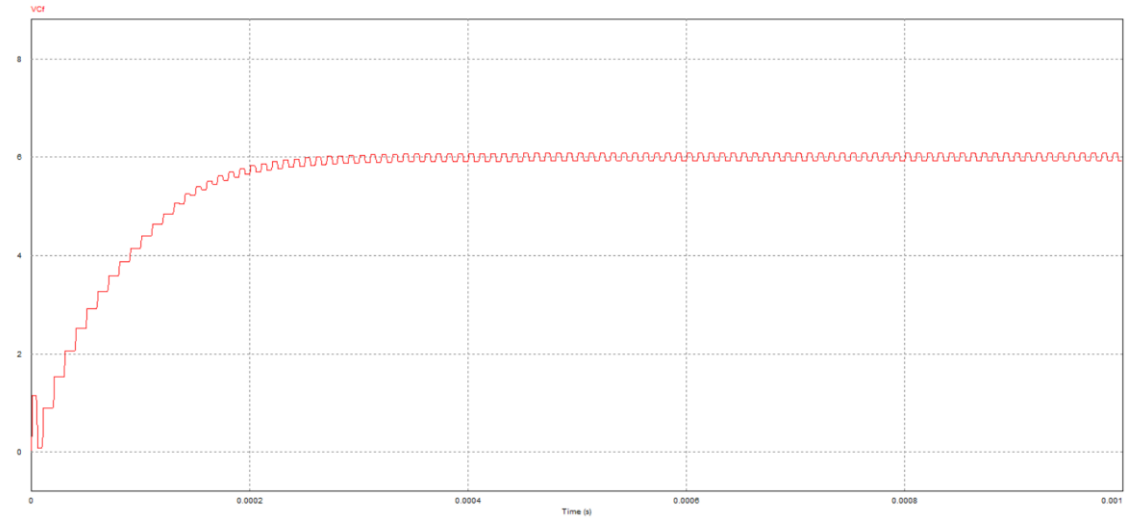

Figure 16: Flying capacitor's voltage showing half of the input voltage showing $½·V_g$.

Once verified that the converter is indeed working as expected, is now ready to be compared with the expression *(33).*

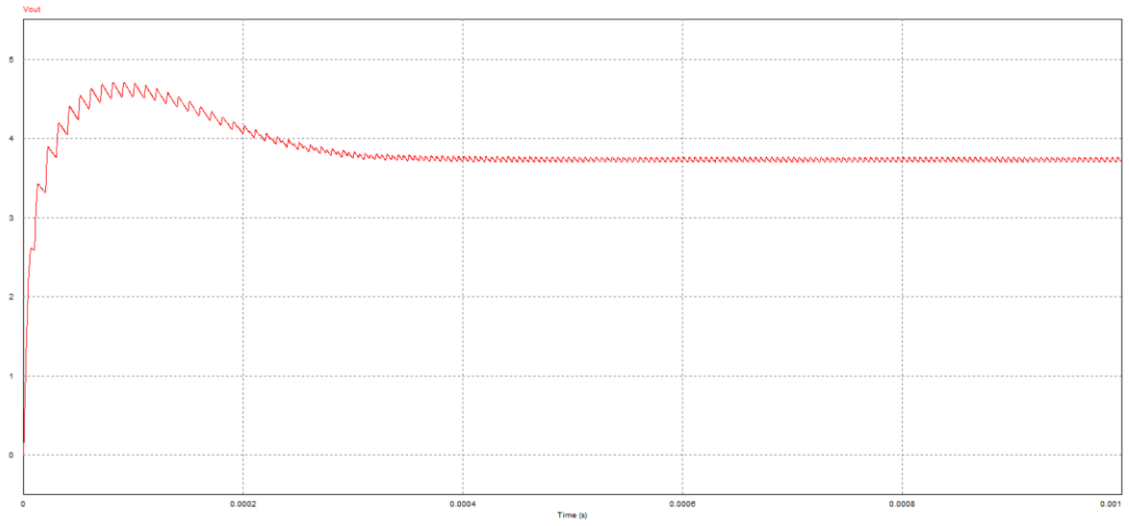

Figure 17: Output voltage with a 12 V input voltage and a duty cycle of 10% and 100 kHz in each MOSFET

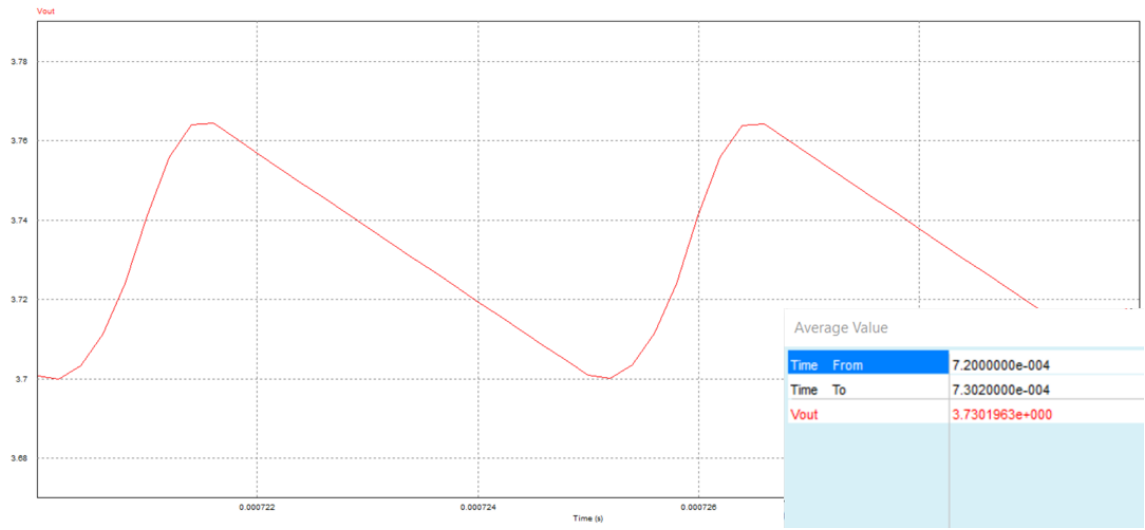

Figure 18: It's the same as Figure 17 but zoomed in. Showing an average output voltage of 3.73 V

To compare it with expression *(33)*, must clarified that since there are two pairs of switches commutating, the frequency and duty cycle considered in *(33)* will be twice the value of the frequency and duty cycle of the square wave used in each MOSFET, however the other parameters will be the same as in *Figure 14*, therefore:

$$V_O = \frac{(0.2)^2 \cdot 12 \cdot \frac{1}{200000} - \sqrt{(0.2)^4 \cdot (12)^2 \left(\frac{1}{200000}\right)^2 + 4 \cdot \frac{4(1 \cdot 10^{-6})}{10} \cdot \frac{(12)^2}{2} \cdot (0.2)^2 \cdot \left(\frac{1}{200000}\right)}}{-2 \cdot \frac{4(1 \cdot 10^{-6})}{10}}$$

$$= 3.71$$

In the simulation the output voltage is 3.73 V and in the mathematical expression is 3.71, this small difference could be easily due the simulation limitations (datapoints) as PSIM demo was used.

3.2 Dynamic model simulation

To verify this model, a bode plot done by PSIM will be compared to the bode plot of expression (38) done with MATLAB.

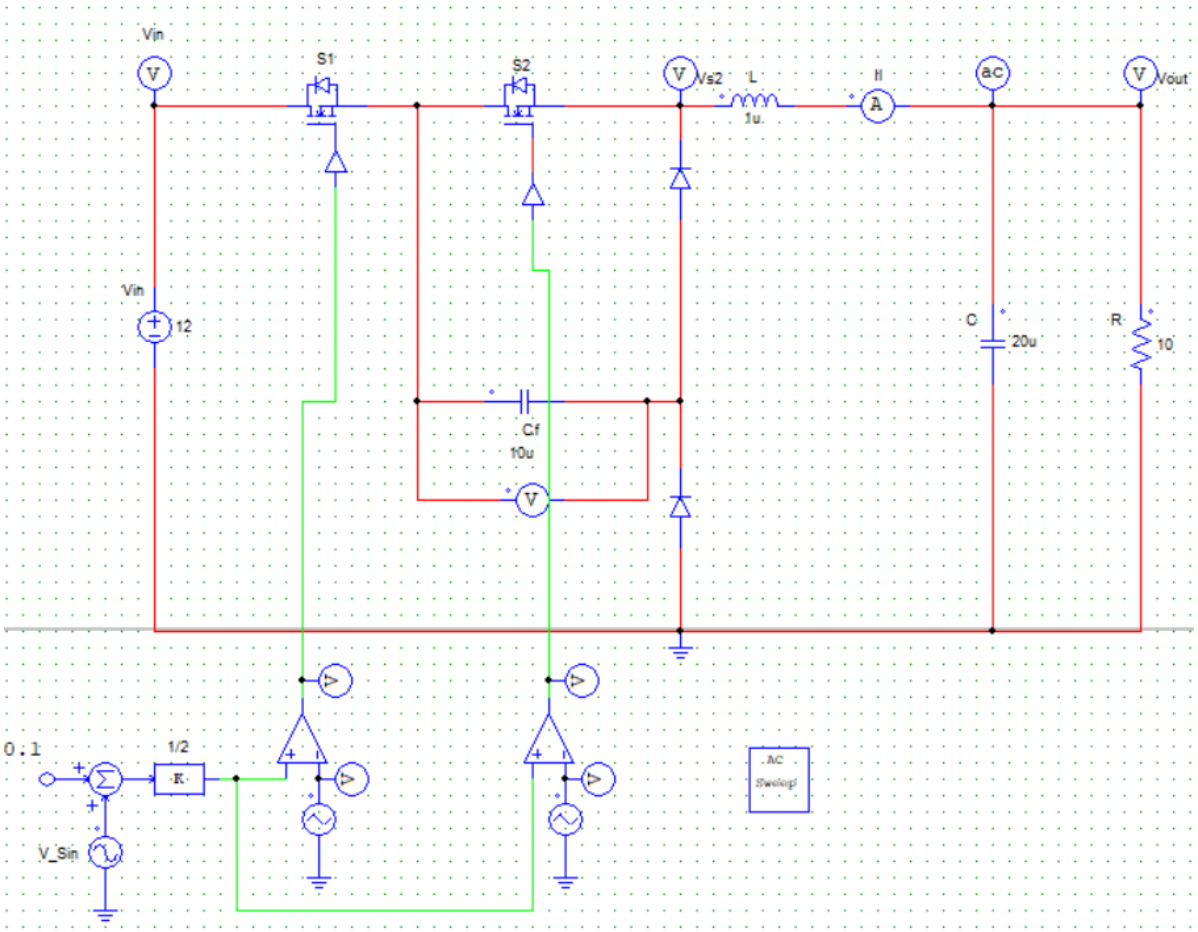

Figure 19: Circuit use to do the bode plot.

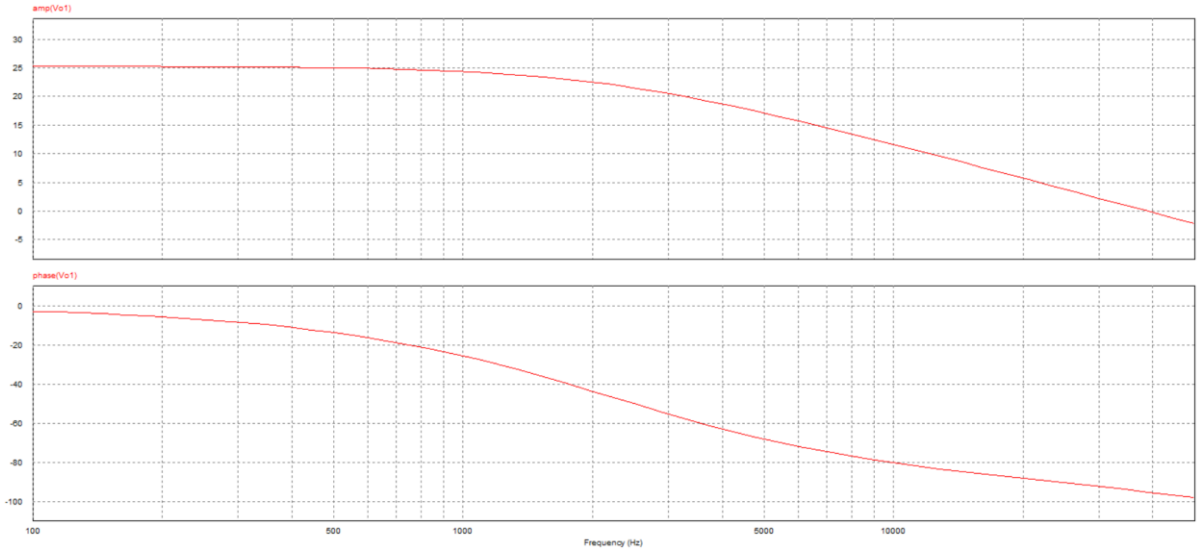

Figure 20: Bode plot of the circuit in Figure 19.

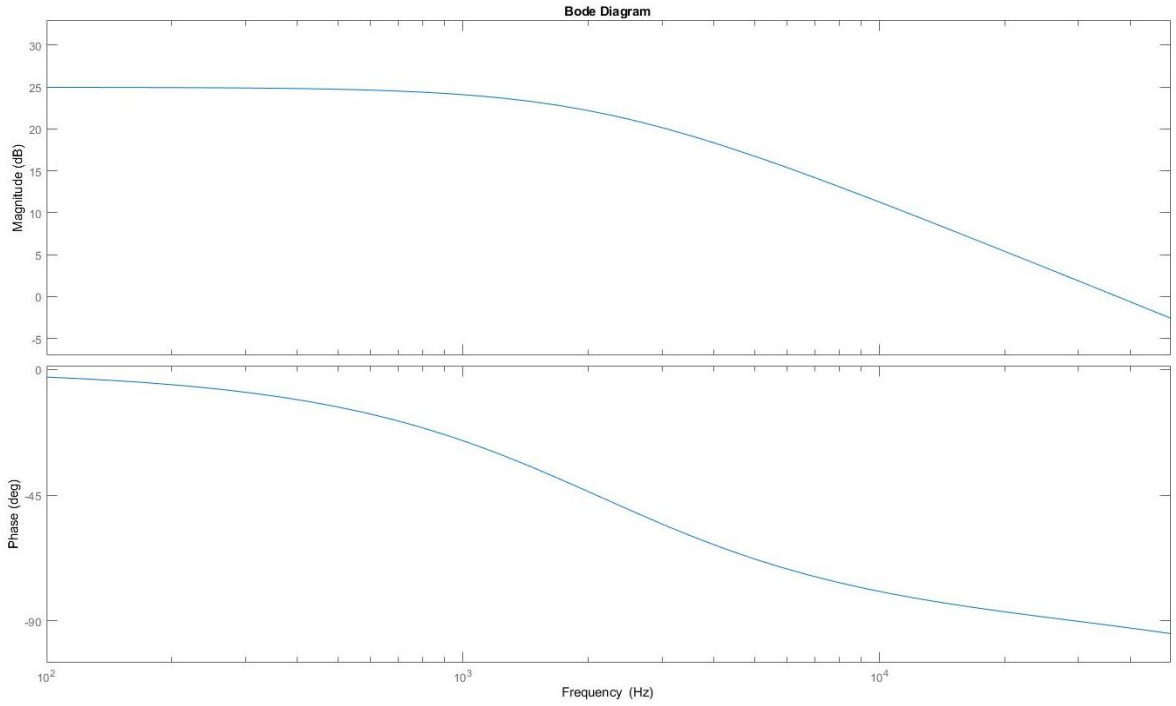

Figure 21: Bode plot of expression (33) done with MATLAB.

As we can see *Figure 21* and *Figure 22* are very similar which concludes that the dynamic model described by expression *(33)* is correct.

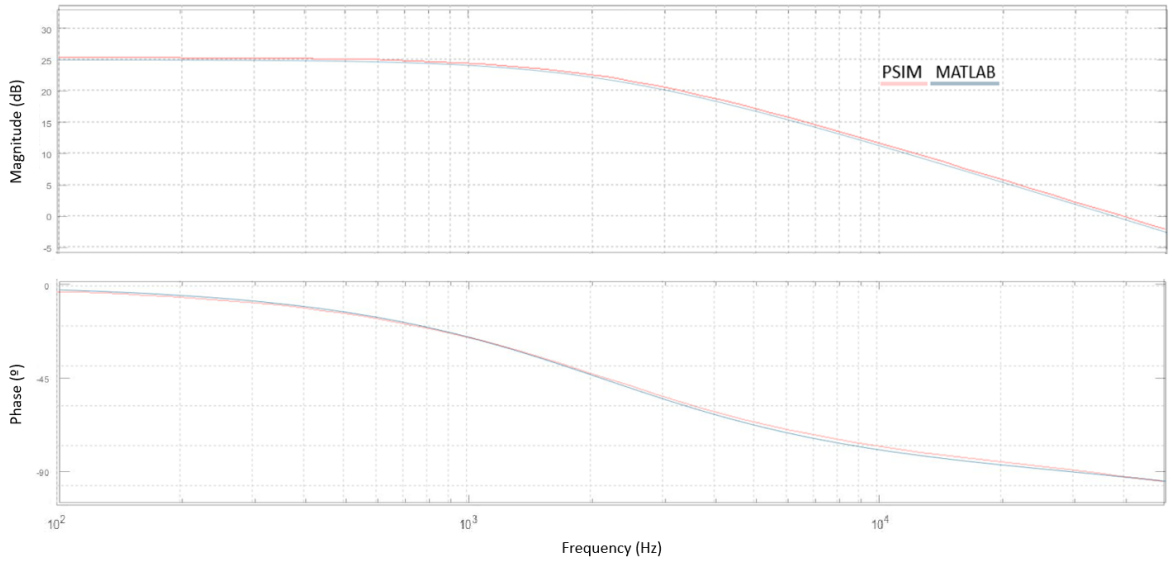

Figure 22: Superposition of Figure 21 and Figure 22

As it can be seen, the two bode plots look the same, therefore the expression *(33)* is proven again to be correct.

4. Voltage-mode control

A PI (Proportional Integral) controller will be designed to be able to regulate with zero steady state error. It will be designed with the help of the bode plot.

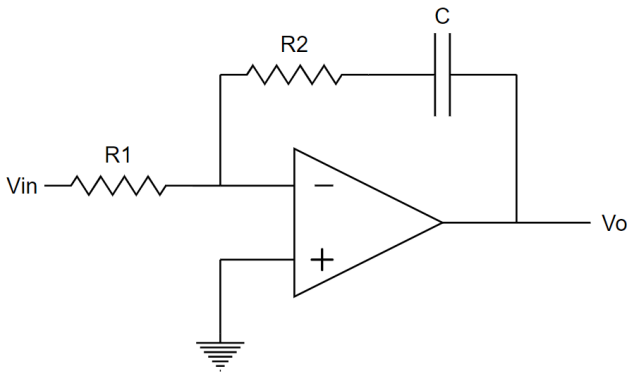

Figure 23: Analog PI controller

In order to have a proper response, a sensed voltage needs to be compared to a reference voltage, in other words, it needs to be compared with the output voltage desired.

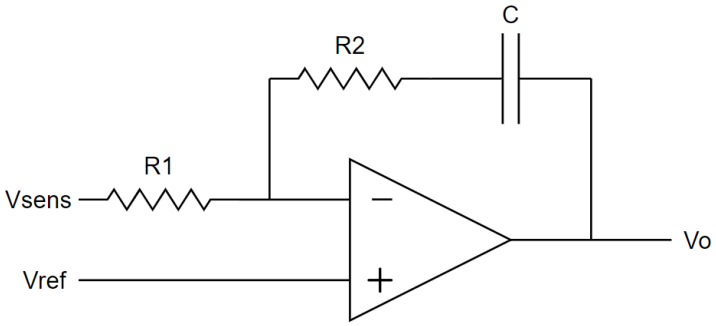

Figure 24: Real PI configuration.

The values for *R1, R2* and *C* must be found in order to have an adequate PI. To find the values, the PI is analysed applying source superposition.

First part of the superposition:

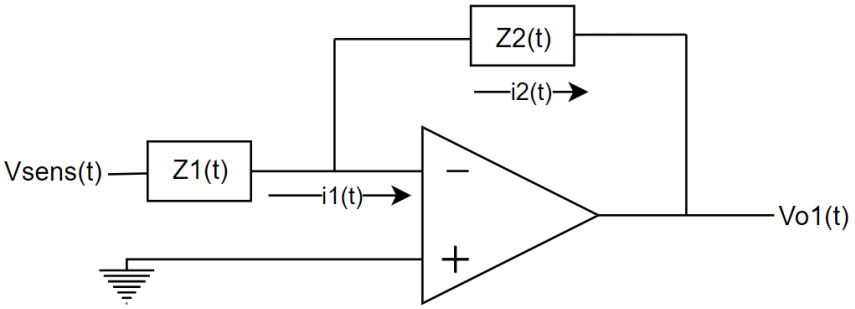

Figure 25: First part of the superposition

Applying virtual short circuit, the following is obtained:

$$i_1(t) = i_2(t)$$

$$\frac{V_{sens}(t)}{Z_1(t)} = -\frac{V_{O1}(t)}{Z_2(t)} \quad \rightarrow \quad \boldsymbol{V_{O1}(t) = -V_{sens}(t)\frac{Z_2(t)}{Z_1(t)}} \tag{39}$$

Second part of the superposition:

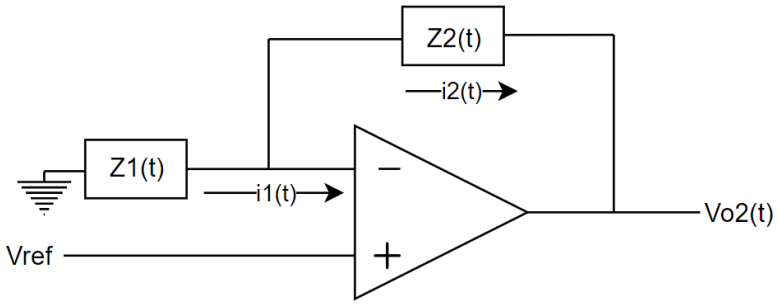

Figure 26: Second part of the superposition.

Applying virtual short circuit, the following is obtained:

$$i_1(t) = i_2(t)$$

$$\frac{-V_{ref}}{Z_1(t)} = \frac{V_{ref} - V_{O2}(t)}{Z_2(t)} \quad \rightarrow \quad \boldsymbol{V_{O2}(t) = V_{ref}\left(1 + \frac{Z_2(t)}{Z_1(t)}\right)} \tag{40}$$

Once analysed both cases of the superposition, the following is left:

$$V_o(t) = V_{O1}(t) + V_{O2}(t) = -V_{sens}(t)\frac{Z_2(t)}{Z_1(t)} + V_{ref}\left(1 + \frac{Z_2(t)}{Z_1(t)}\right)$$

$\mathcal{L}$:

$$Vo(s) =) = -V_{sens}(s)\frac{Z_2(t)}{Z_1(t)} + \frac{V_{ref}}{s}\left(1 + \frac{Z_2(t)}{Z_1(t)}\right)$$

Since only the incremental part is what is wanted and V_{ref} is a constant value, the following is left:

$$\frac{\hat{V}_O}{\hat{V}_{sens}} = -\frac{Z_2(t)}{Z_1(t)} \quad \textbf{(41)}$$

Knowing that $Z_1(s)=R_1$ and $Z_2(s)=R_2 + 1/Cs$, the following is left:

$$\frac{\hat{V}_O}{\hat{V}_{sens}} = -\frac{R_2 + \frac{1}{Cs}}{R_1} = -\frac{R_2Cs + 1}{R_1Cs} = -\frac{s + \frac{1}{R_2C}}{\frac{R_1Cs}{R_2C}} \quad \textbf{(42)}$$

Is known that general formula for a PI controller is:

$$G_C(s) = \frac{K(s + z_1)}{s} \quad \textbf{(43)}$$

If *(42)* and *(43)* are compared, what is left is:

$$K = \frac{R_2}{R_1} \qquad and \qquad z_1 = \frac{1}{R_2C} \quad \textbf{(44)}$$

First of all z_1 must be found, it's found by using the argument condition, for this PI a phase margin of 60º has been chosen so those 60º need to be considered:

$$T(s) = G_C(s)G(s) \quad where \quad G_C(s) \equiv PI\ controller \quad G(s) \equiv \frac{\hat{y}(s)}{\hat{d}_1(s)}$$

From expression *(33)* and with the use of MATLAB, the poles have been found, one of them is at $2.55 \cdot 10^6$ rad/s and the other one is at $0.001 \cdot 10^6$ rad/s.

$$-180º + 60º = -90º - \tan^{-1}\left(\frac{\omega_g}{2.55 \cdot 10^{-6}}\right) - \tan^{-1}\left(\frac{\omega_g}{0.01 \cdot 10^{-6}}\right) + \tan^{-1}\left(\frac{\omega_g}{z_1}\right) \quad \textbf{(45)}$$

ω_g is the imaginary part of the desired poles

Where ω_g will have a value of one decade below the switching frequency, in this case the commutation frequency is 200 kHz, therefore, ω_g = 20 kHz = $1.27 \cdot 10^5$ rad/s. With expression *(44)* and all the information above, it can be seen how the zero (z_1) will be placed at $7.83 \cdot 10^4$ rad/s. Now with the help of MATLAB the value for *K* is found.

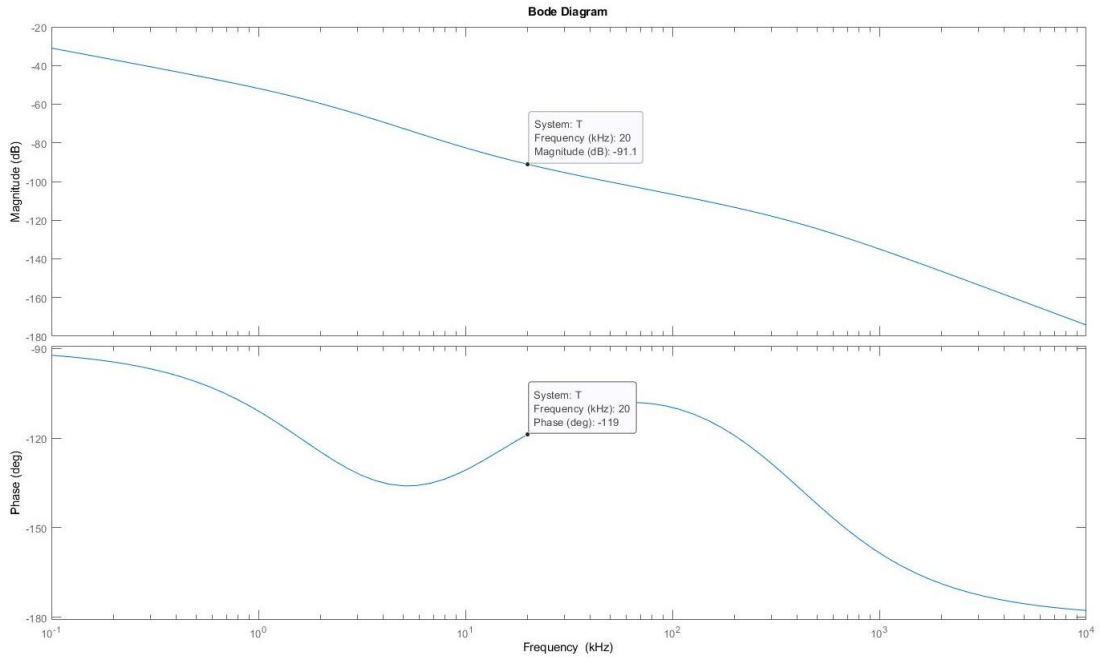

Figure 27: Bode plot of GC(s)G(s) without K

Looking at *Figure 28,* when the phase is -120º, which is where 0 dB is wanted to have the 60ª phase margin, the magnitude is -91.1 dB, knowing this, the value of *K* can be found since it has to compensate those -91.1 dB.

$$20log_{10}(K) = 91.1\ dB \quad \therefore K = 35890$$

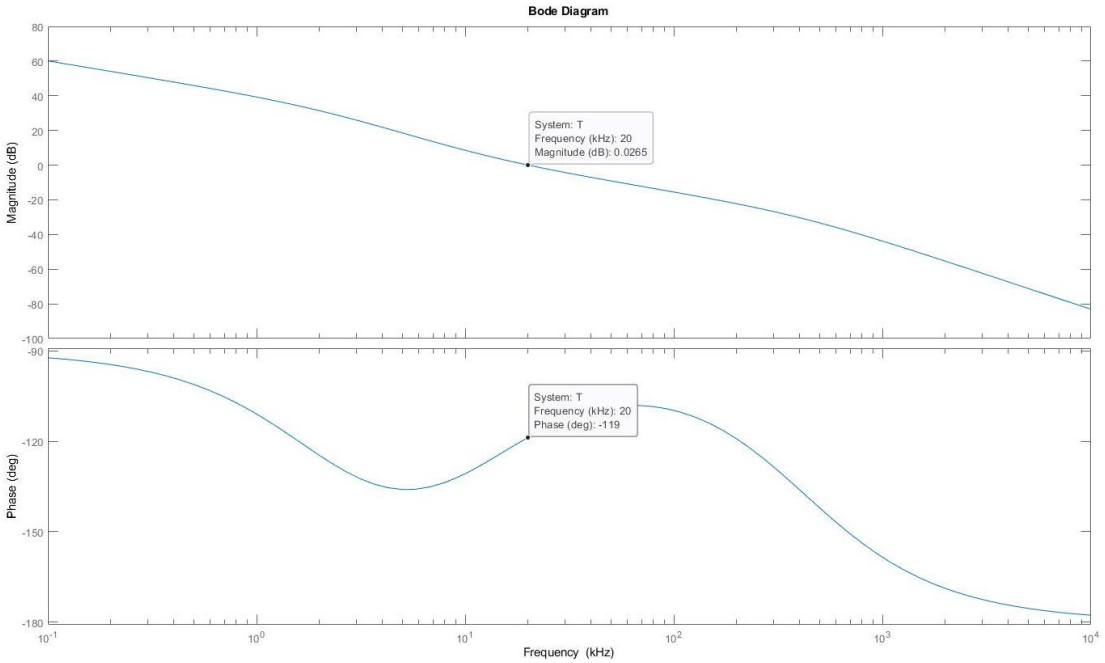

Figure 28: Bode plot of GC(s)G(s) with K

Now looking at *Figure 29,* it can be seen how the controller meets the established requirements. Now with this information, the values of the controller's parameters can be found using expression *(44)* leaving that:

$$R_1 = \frac{R_2}{35890} \qquad and \qquad R_2 = \frac{1}{7.83 \cdot 10^4 \cdot C}$$

Using standardized values, the parameters have the following values:

$$C = 100\mu F \qquad R_1 = 0.00022\Omega \qquad R_2 = 8.2\Omega$$

It needs to be clarified, that those values are only applicable for the following simulation, where a tension sensor is used, in a real-life case, a different set up should be used, for example using a buffer amplifier or using a voltage divider and higher value resistors to avoid "stealing current" from the load.

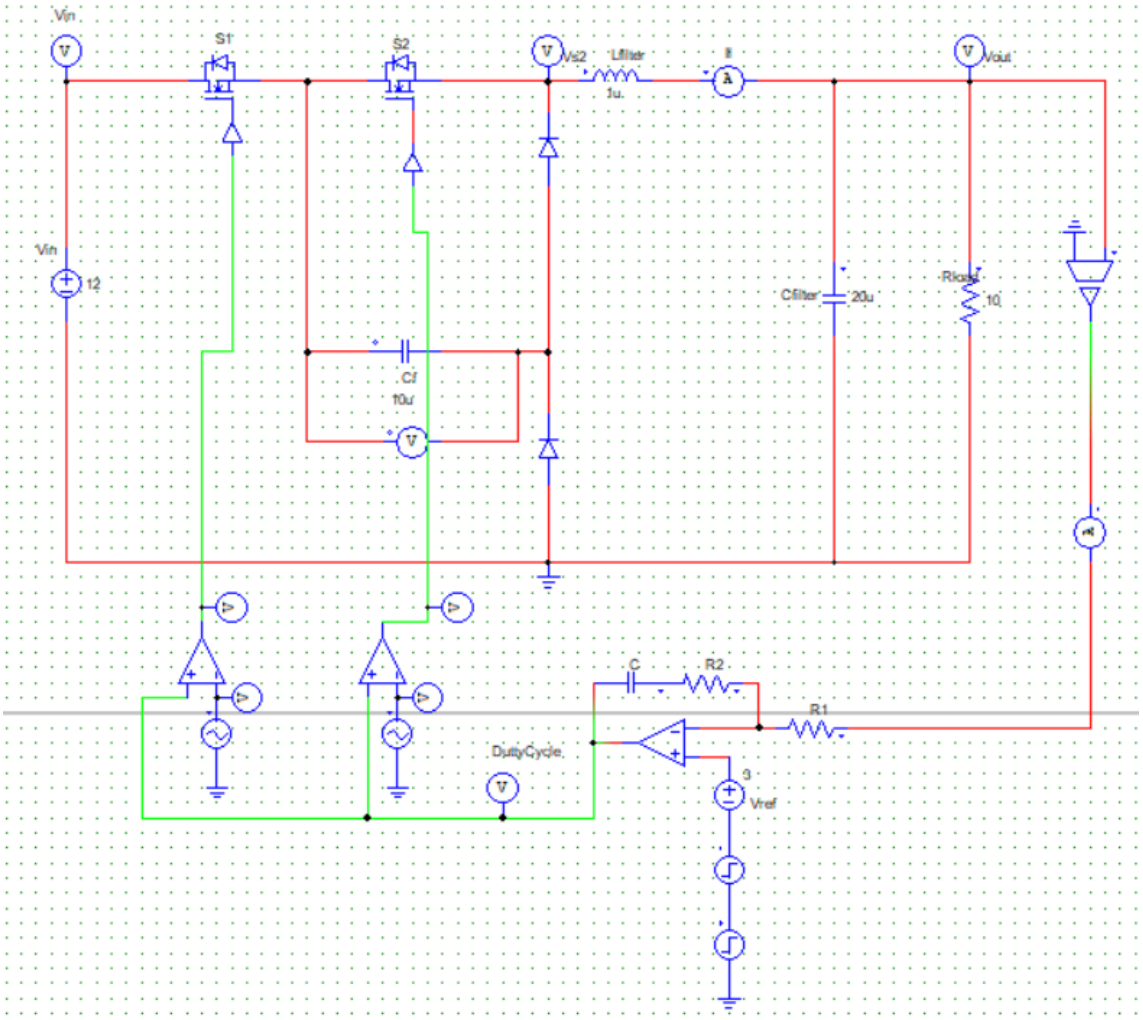

Figure 29: Circuit used in PSIM for the PI simulation.

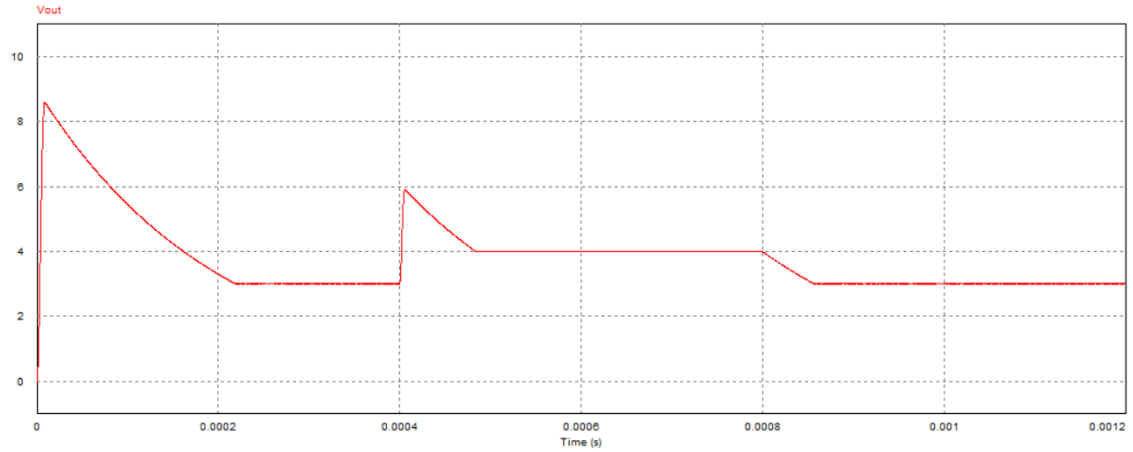

Figure 30: Converter's response with a 3V order with a ±1V perturbation.

5. Prototype

At the laboratory, a prototype of the power stage has been built and tested, the following components have been used in order to build it:

Table 2: Components used for the protype

Component	Number to refer on *Figure 30*	RS Code
Matrix board	1	518-6610
Schottky Diode	2	917-9120
MOSFET driver	3	260-5179
Switching diode	4	842-8002
Ceramic capacitor 10 μF	5	242-7563
Inductor 1 μH	6	715-7131
Resistor 10 Ω	7	707-8782
Resistor 5 Ω	8	158-503
Resistor 4.7 Ω	9	157-544
MOSFET	10	914-8154

Some components such as the connectors and the decoupling capacitors placed at the connectors and the drivers, were directly obtained from the laboratory and unfortunately there is no RS code for reference.

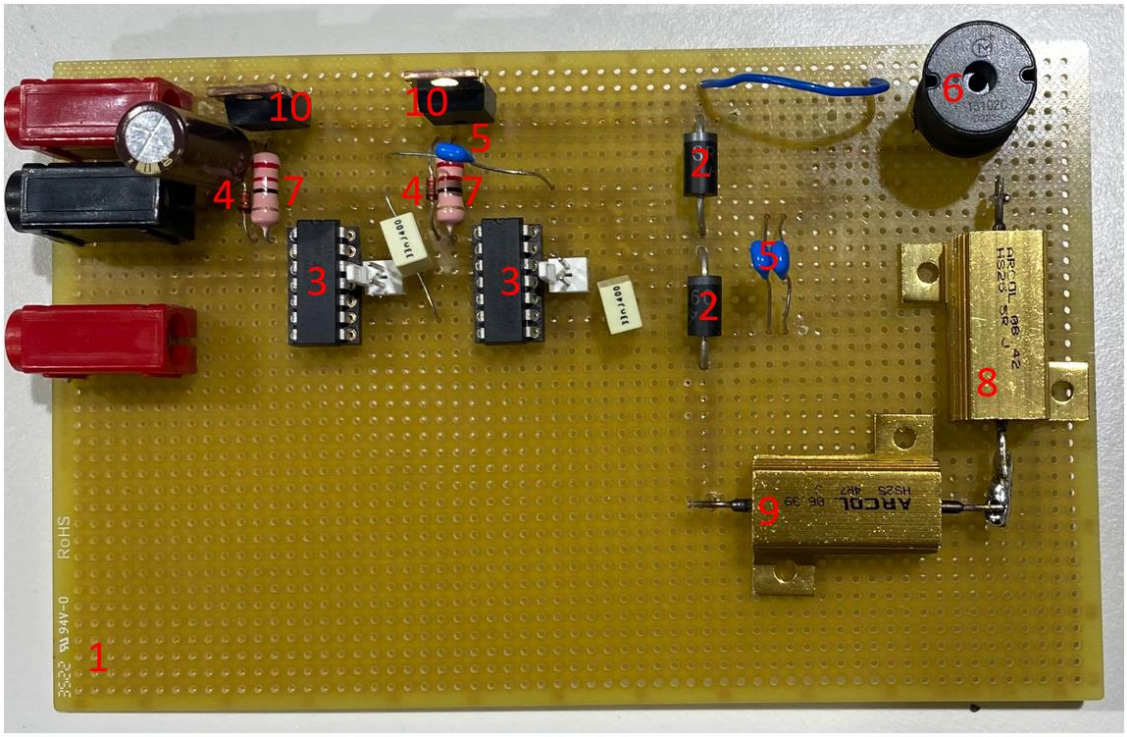

Figure 31: Top view of the prototype.

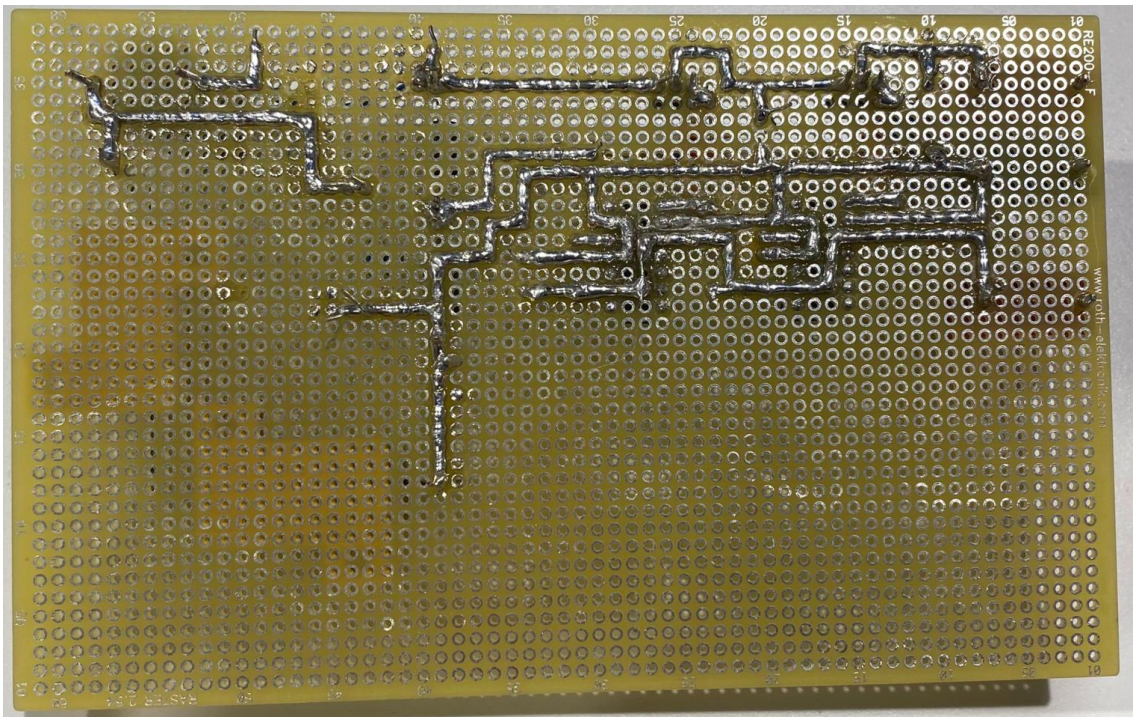

Figure 32: Bottom view of the prototype.

5.1 Prototype testing

To know if the protype built is working properly, some testing needs to be done, therefore, some measurements need to be taken. For this protype, measurements such

as, input voltage, output voltage, inductor's current, MOSFET's gate to source voltage and flying capacitor's voltage have been measured with an oscilloscope.

5.1.1 Current probe adjustment

To measure the current there has been the need to adjust the current probe properly, since the current probe cannot be used as straight forward as the voltage probe, the adjustment has been done by short circuiting the voltage source with a known current, and adjusting the gain of the oscilloscope manually until the reading matches the known current.

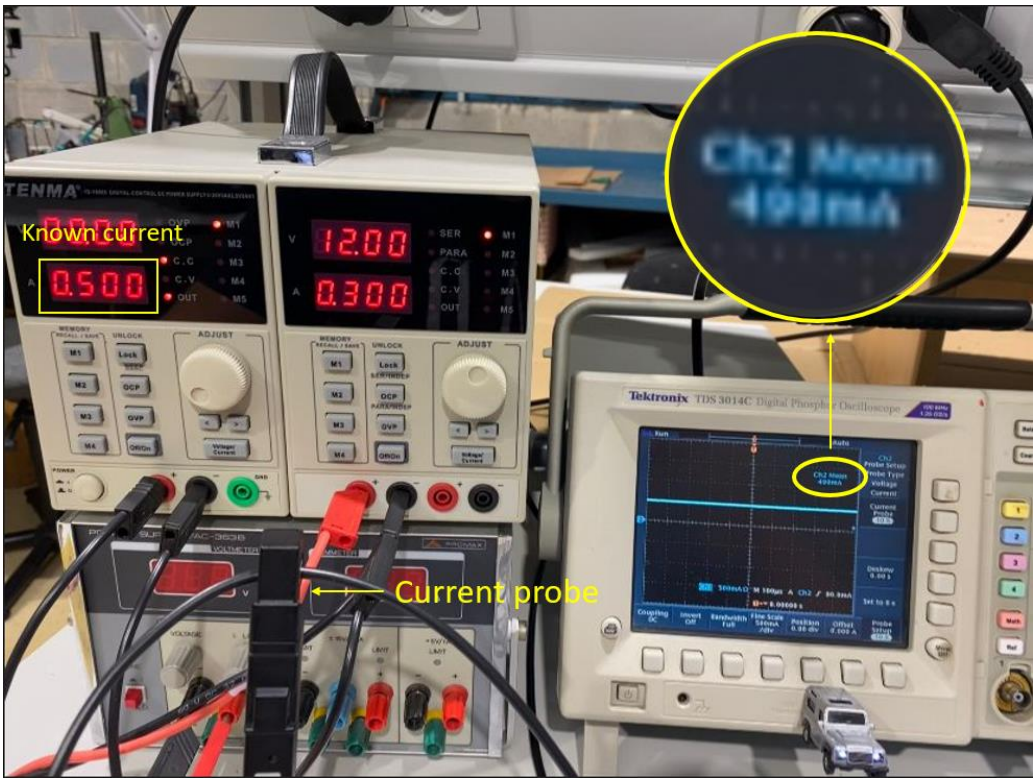

Figure 33: First checking of the current probe

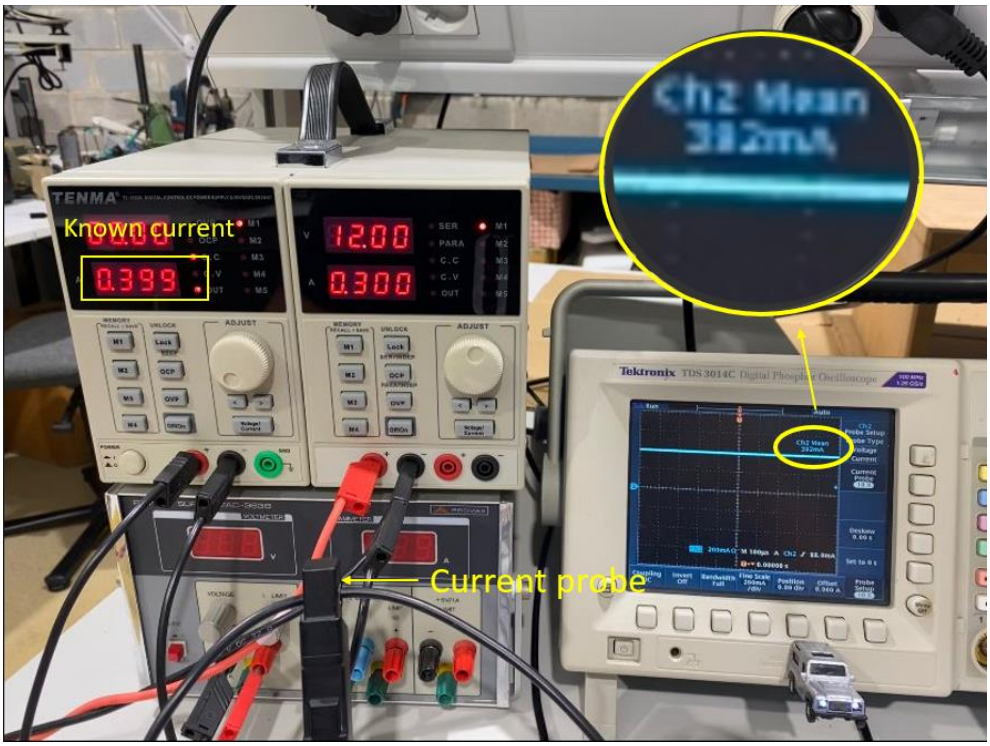

Figure 34: Second checking of the current probe

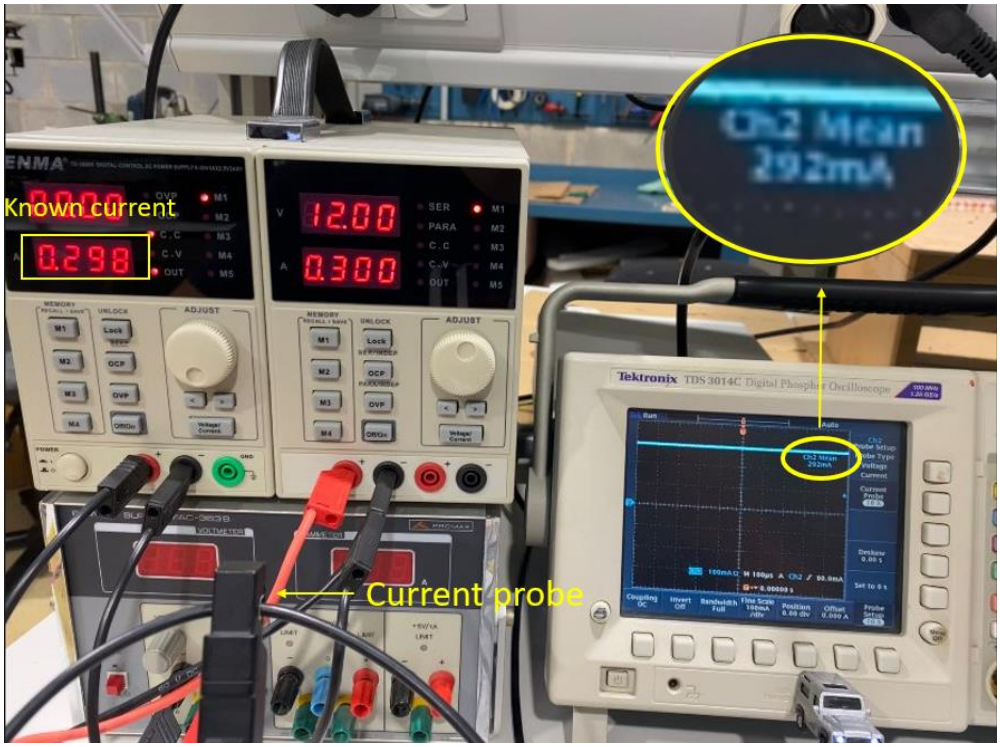

Figure 35: Third checking of the current probe

Look back to *Figure 34, Figure 35* and *Figure 36*, it can be appreciated that the probe measurements are going to be quite accurate throughout the prototype's testing.

5.1.2Measurements

The measurements mentioned above, have been taken four times, for four different duty cycles (the duty cycles of the PWM signal that arrives to the MOSFET are half of that percentage), 10%, 20%, 30% and 50%.

5.1.2.1 Output

5.1.2.1.1 Five percent of duty cycle

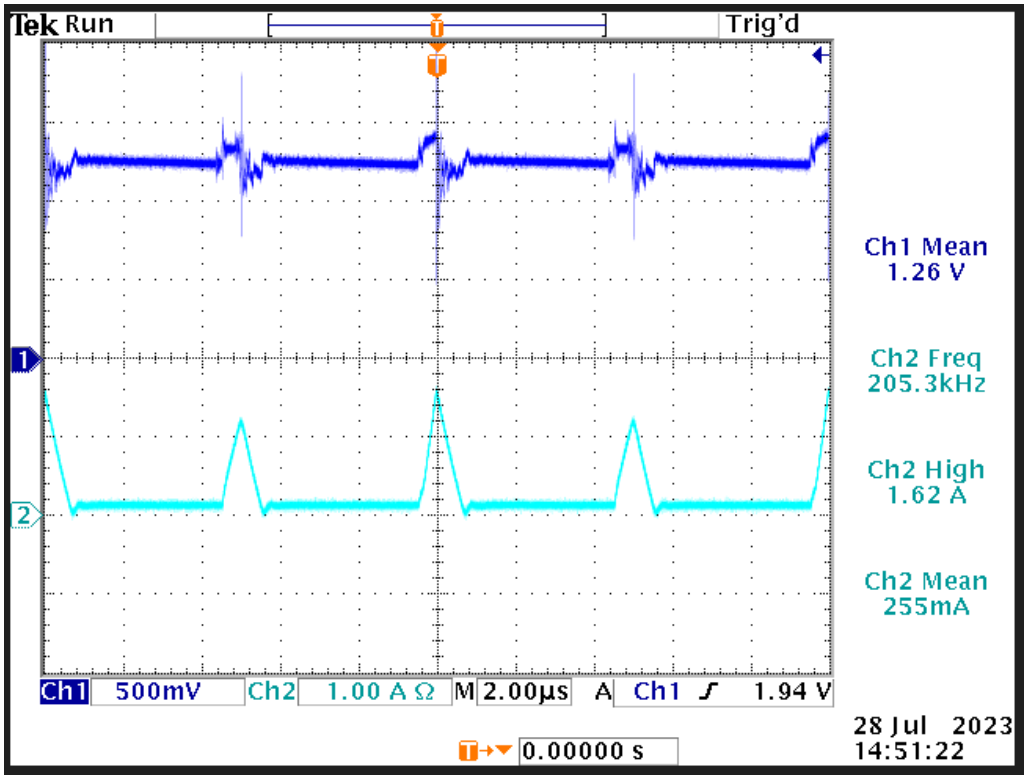

Figure 36: Real output voltage (Ch1) and output current (Ch2)

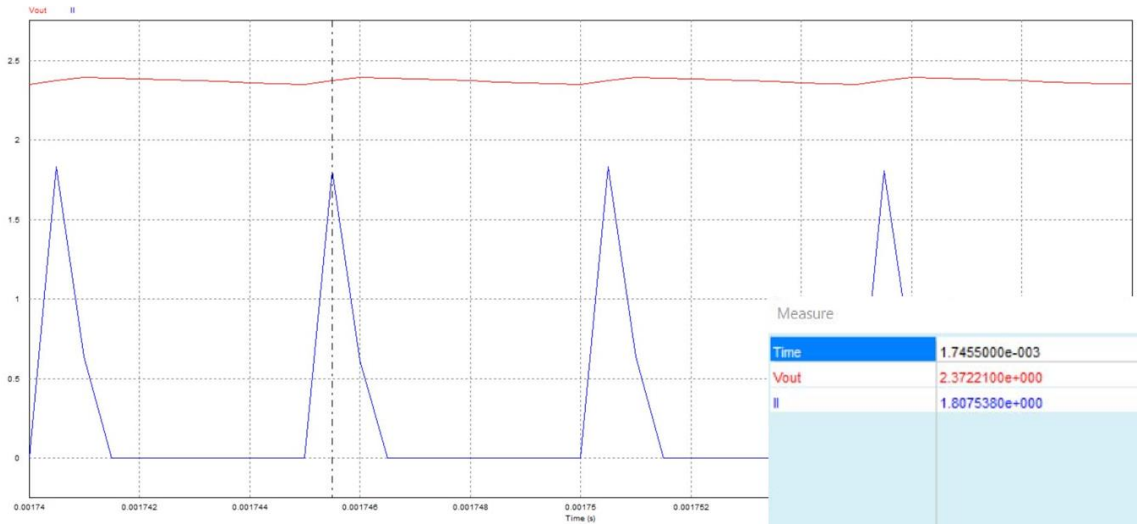

Figure 37: Simulated (peak values) output voltage (red) and output current (blue)

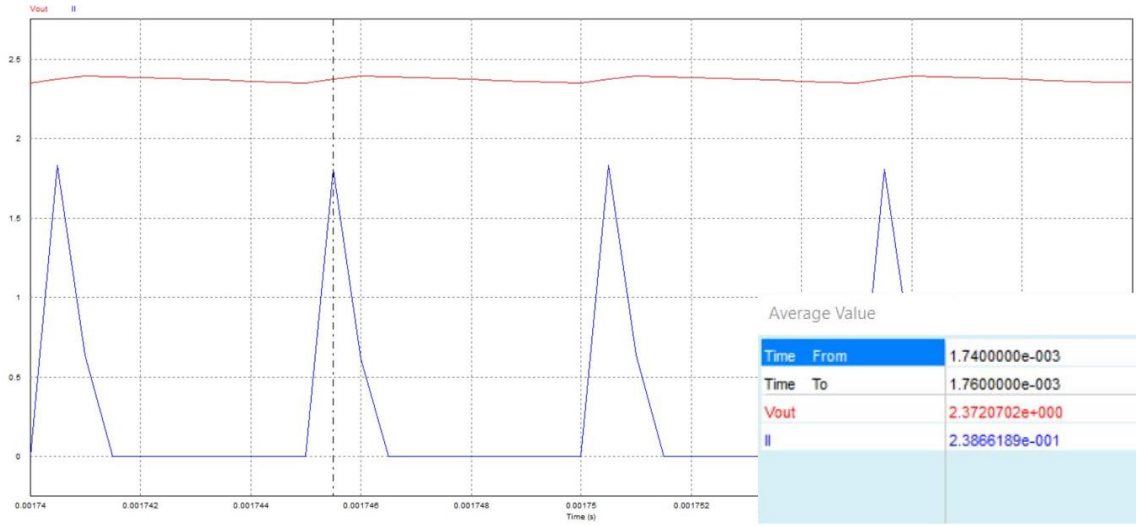

Figure 38: Simulated (mean values) output voltage (red) and output current (blue)

5.1.2.1.2 Ten percent of duty cycle

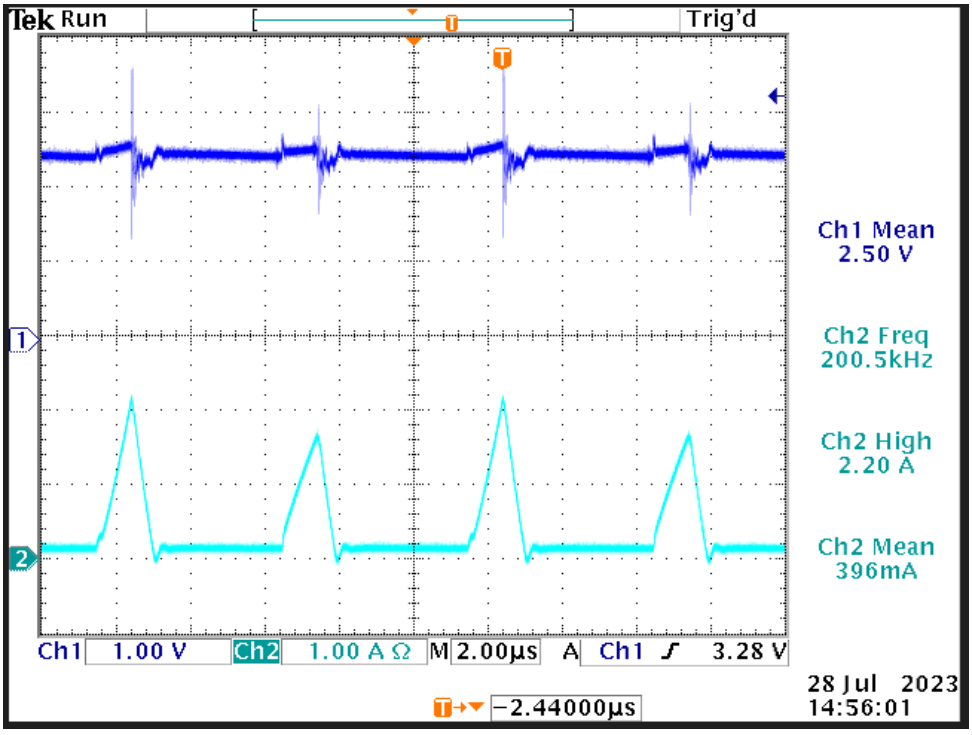

Figure 39: Real output voltage (Ch1) and output current (Ch2)

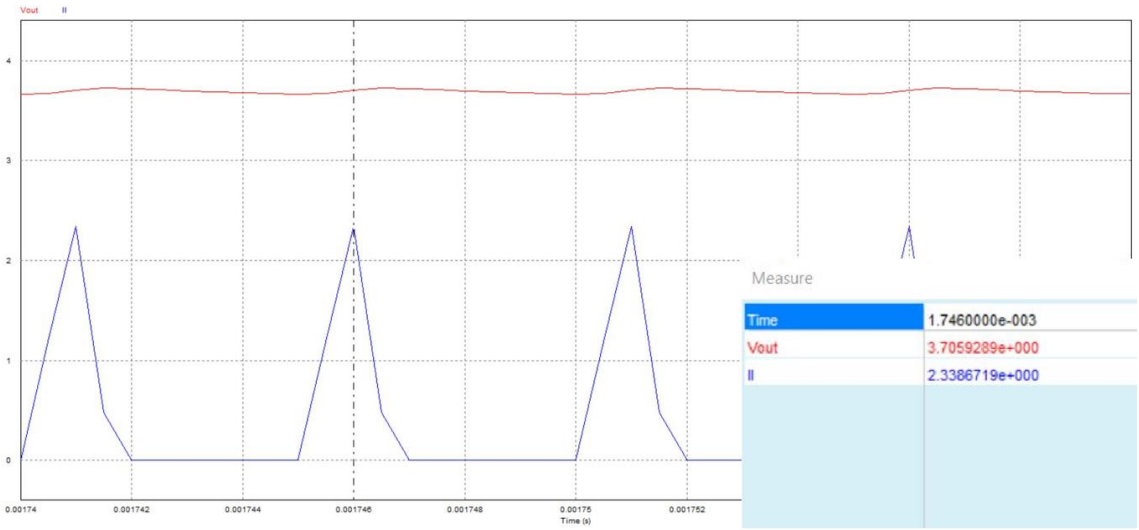

Figure 40: Simulated (peak values) output voltage (red) and output current (blue)

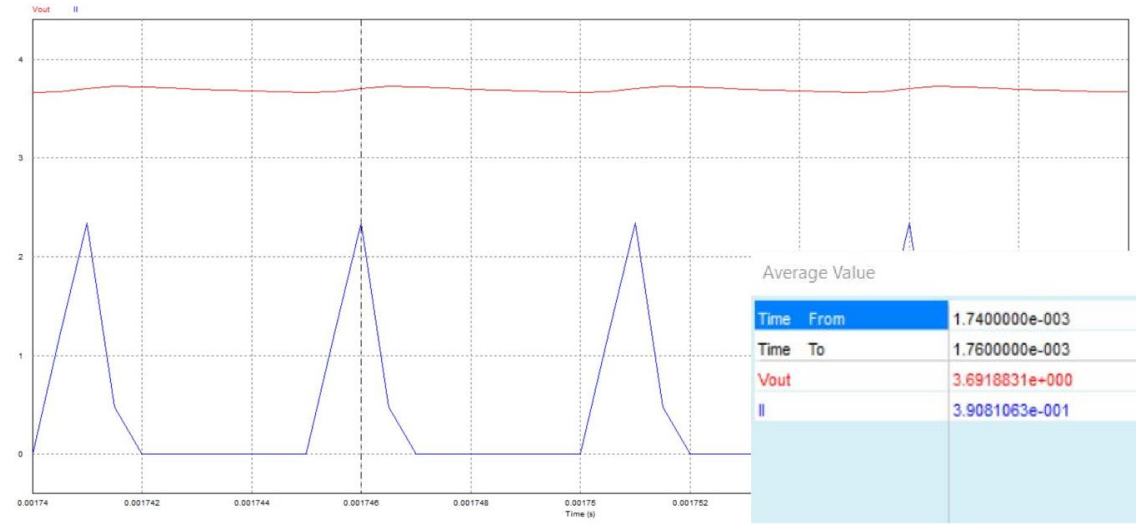

Figure 41: Simulated (mean values) output voltage (red) and output current (blue)

5.1.2.1.3 Fifteen percent of duty cycle

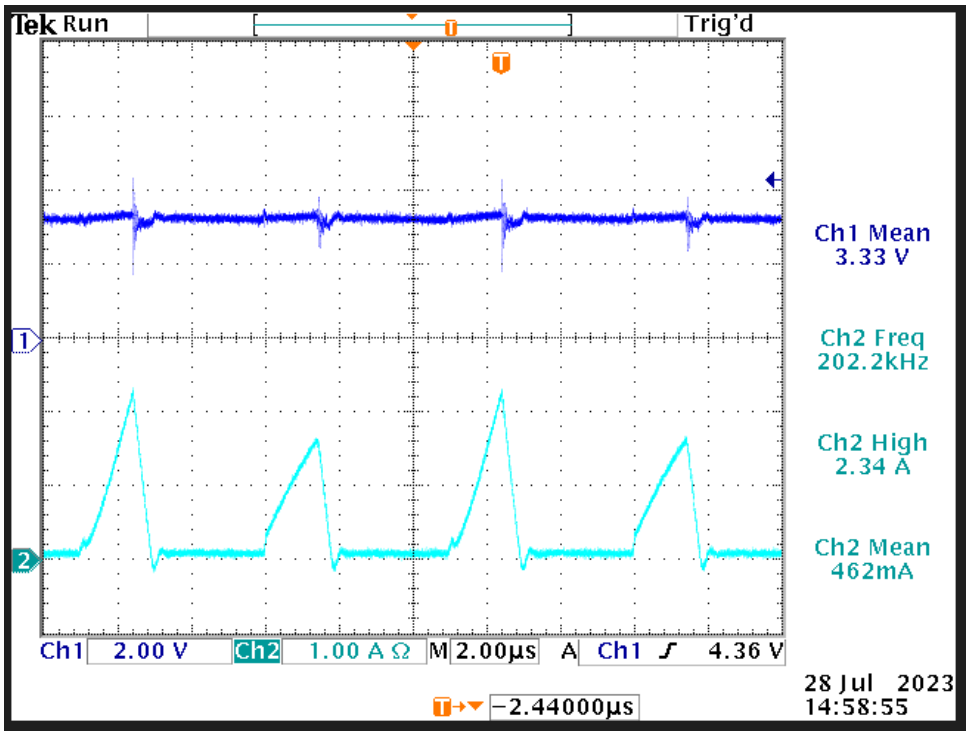

Figure 42: Real output voltage (Ch1) and output current (Ch2)

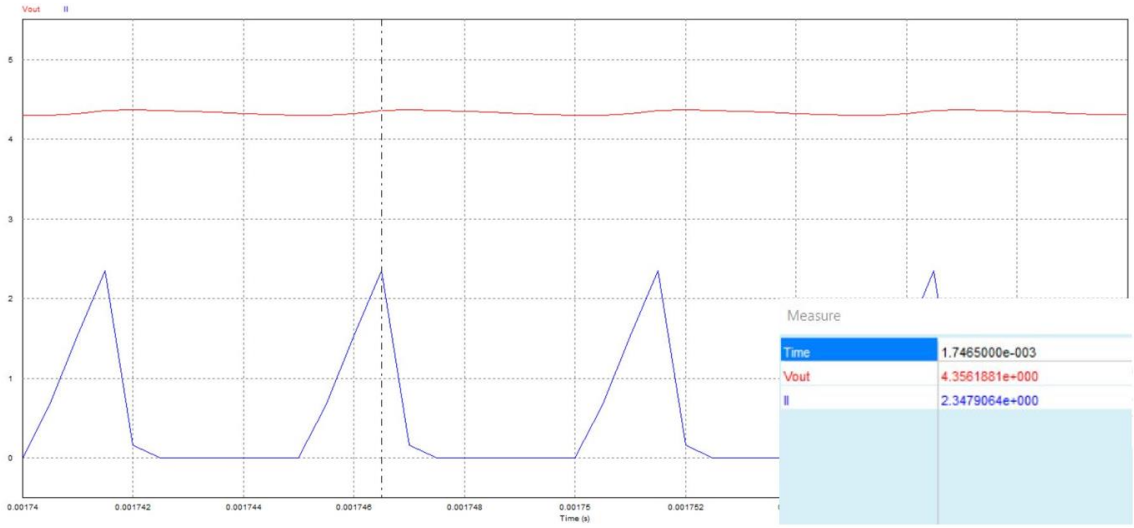

Figure 43: Simulated (peak values) output voltage (red) and output current (blue)

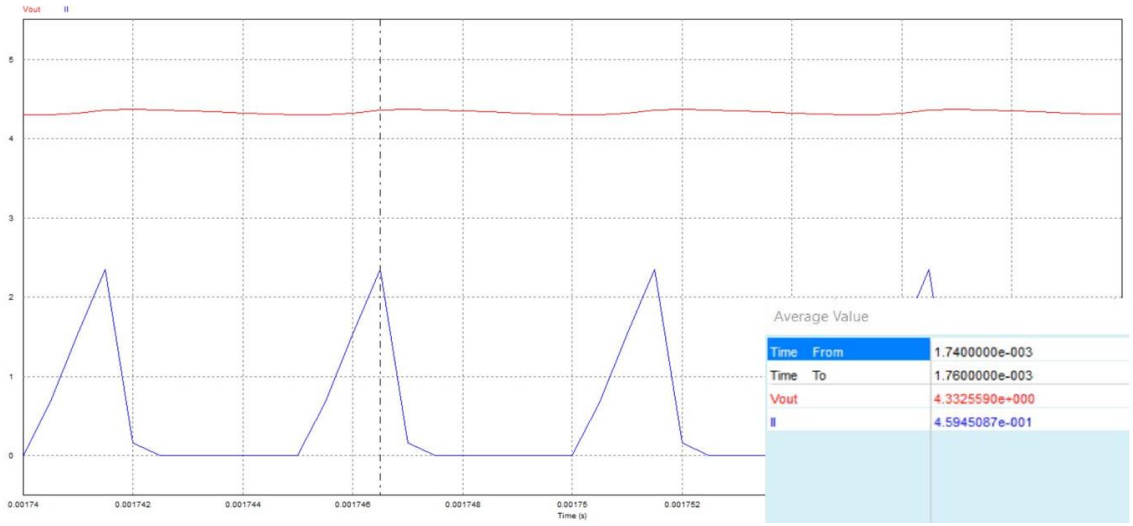

Figure 44: Simulated (mean values) output voltage (red) and output current (blue)

5.1.2.1.4 Twenty percent of duty cycle

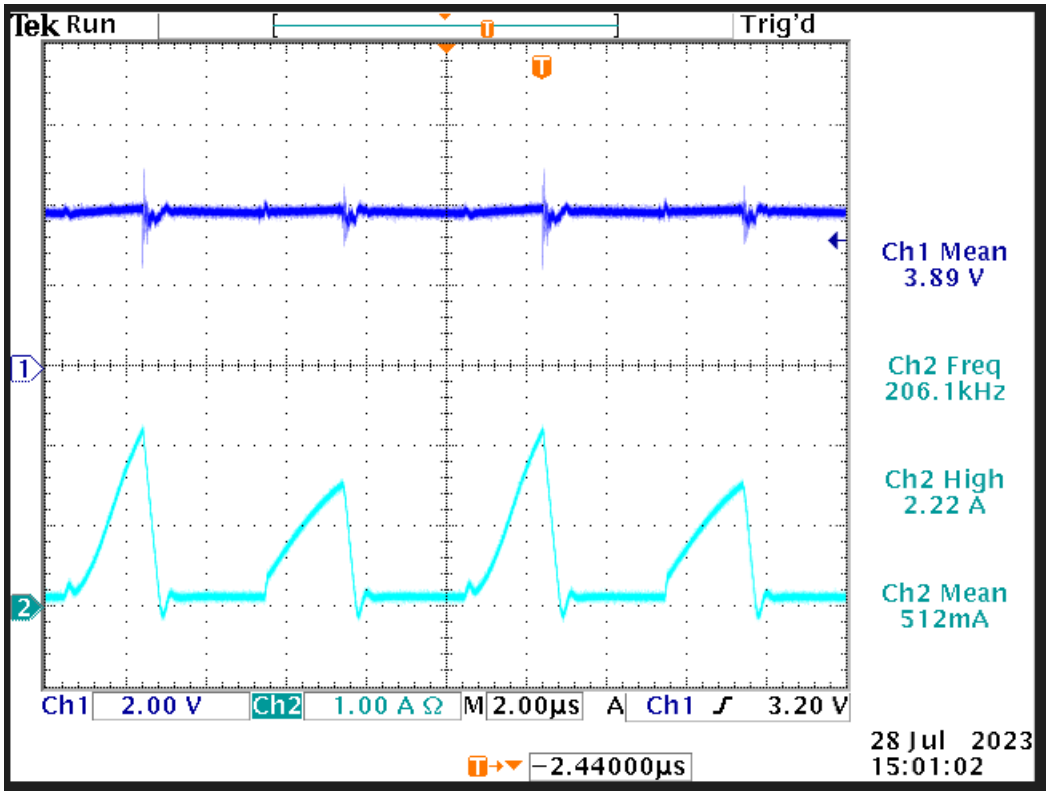

Figure 45: Real output voltage (Ch1) and output current (Ch2)

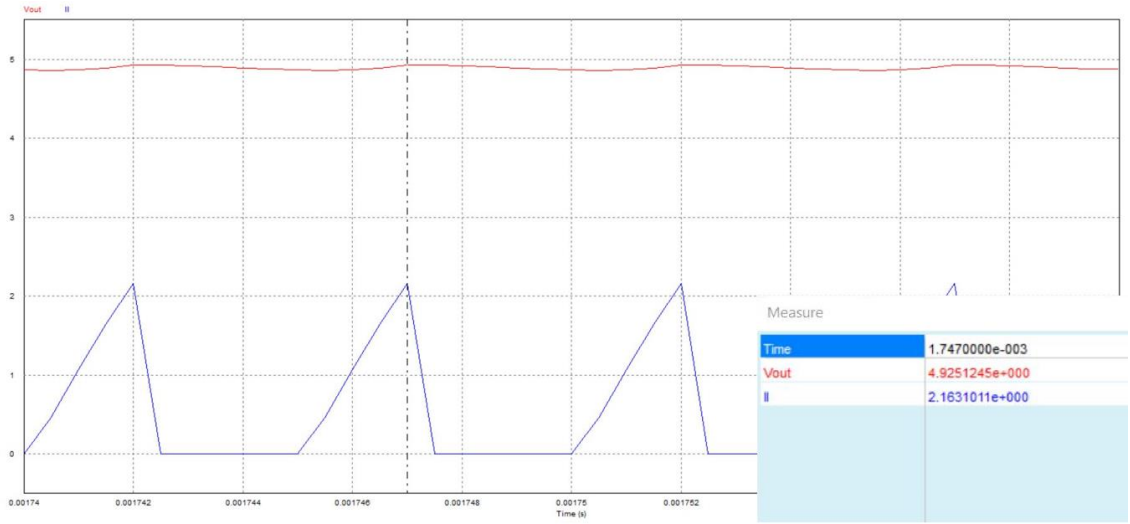

Figure 46: Simulated (peak values) output voltage (red) and output current (blue)

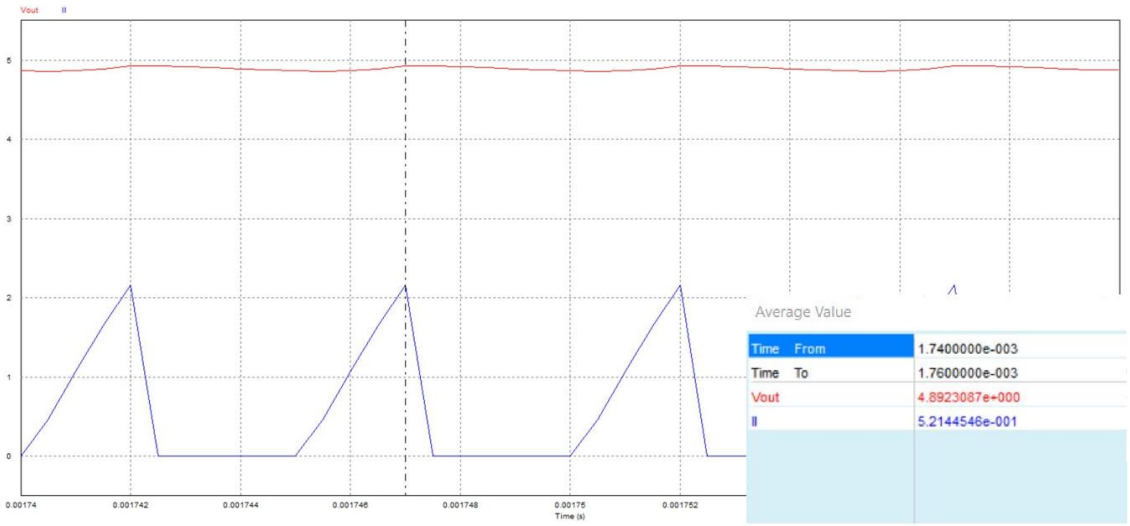

Figure 47: Simulated (mean values) output voltage (red) and output current (blue).

In the previous sections, can be appreciated how the real measurements compared to the simulated ones are very similar, the differences are that the real output voltage has a lot of noise due the imperfect weldings, the current's shapes are similar as well, but a pattern can be observed where every other peak there is a decrease in the maximum current value.

The reason of that pattern could be done due variations in the flying capacitor's voltage, referring to expression *(5),* it can be seen how this can affect the inductor's current slope directly.

To see a clearer comparison, the following table contains all the relevant data from the pictures above:

Table 3: Measurements summary

Duty cycle (%)	Real peak current (A)	Simulated peak current (A)	Real mean current (mA)	Simulated mean current (mA)	Real mean voltage (V)	Simulated mean voltage (V)
5	1.62	1.81	255	239	1.26	2.37
10	2.20	2.33	396	391	2.50	3.69
15	2.34	2.34	462	459	3.33	4.33
20	2.22	2.16	512	521	3.89	4.89

Looking at *Table 3*, can be concluded that in general, the converter is behaving as expected, the mean output voltage is lower in the real case compared to the simulation, this makes a lot of sense, since in the simulation it's an ideal case, therefore no losses were considered. The same logic is applied when comparing the peak current values of both cases, nevertheless the mean value is higher in real life than in the simulation due the pattern problem mentioned earlier.

5.1.2.2 MOSFET's gate to source voltage

5.1.2.2.1 Five percent of duty cycle

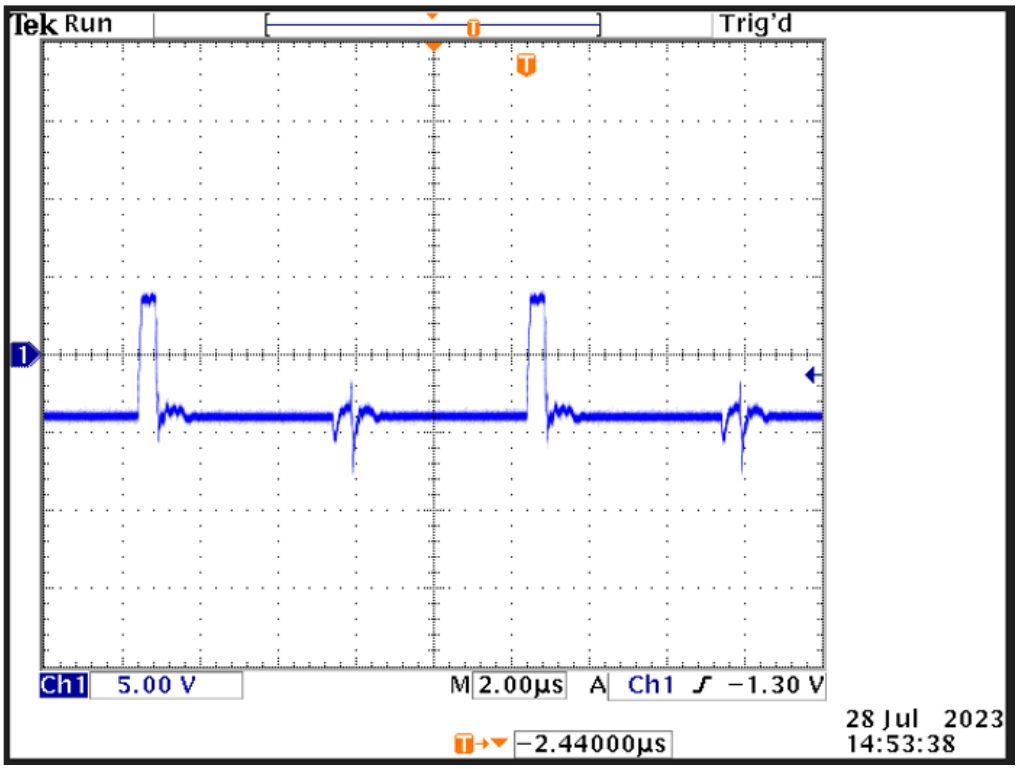

Figure 48: MOSFET's gate to source voltage

5.1.2.2.2 Ten percent of duty cycle

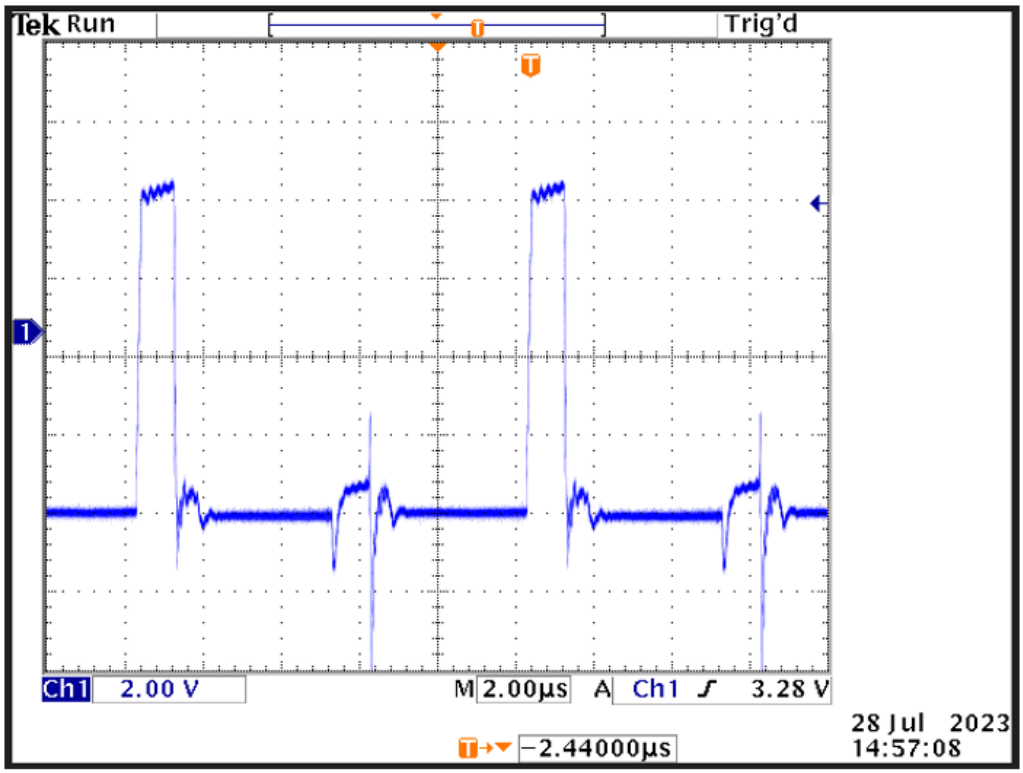

Figure 49: MOSFET's gate to source voltage

5.1.2.2.3 Fifteen percent of duty cycle

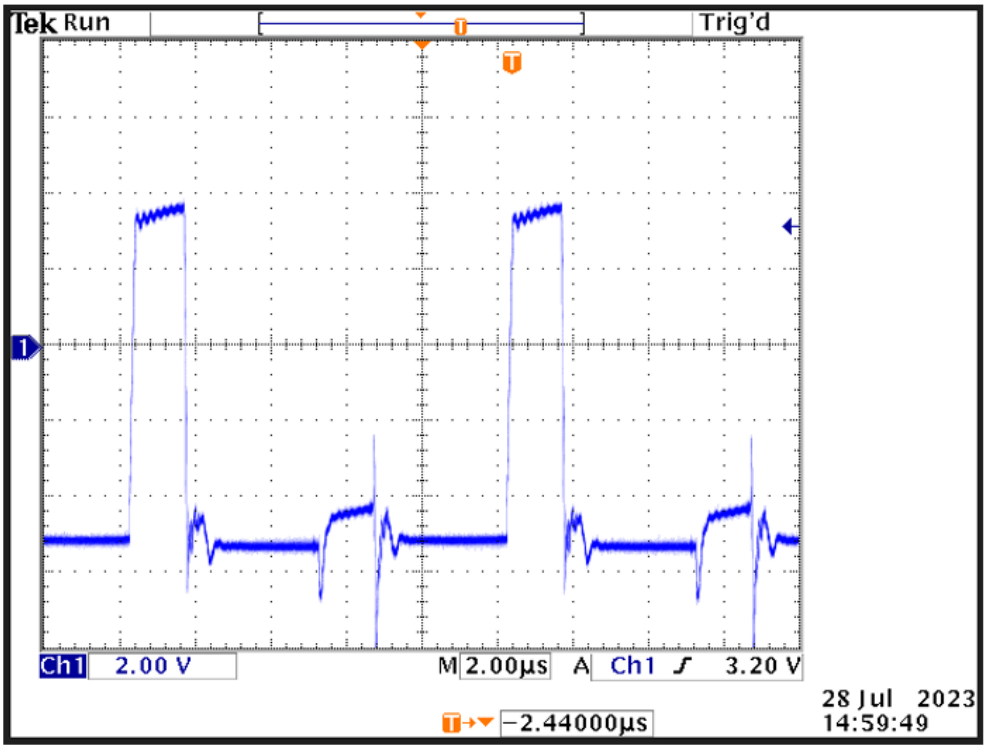

Figure 50: MOSFET's gate to source voltage.

5.1.2.2.4 Twenty percent of duty cycle

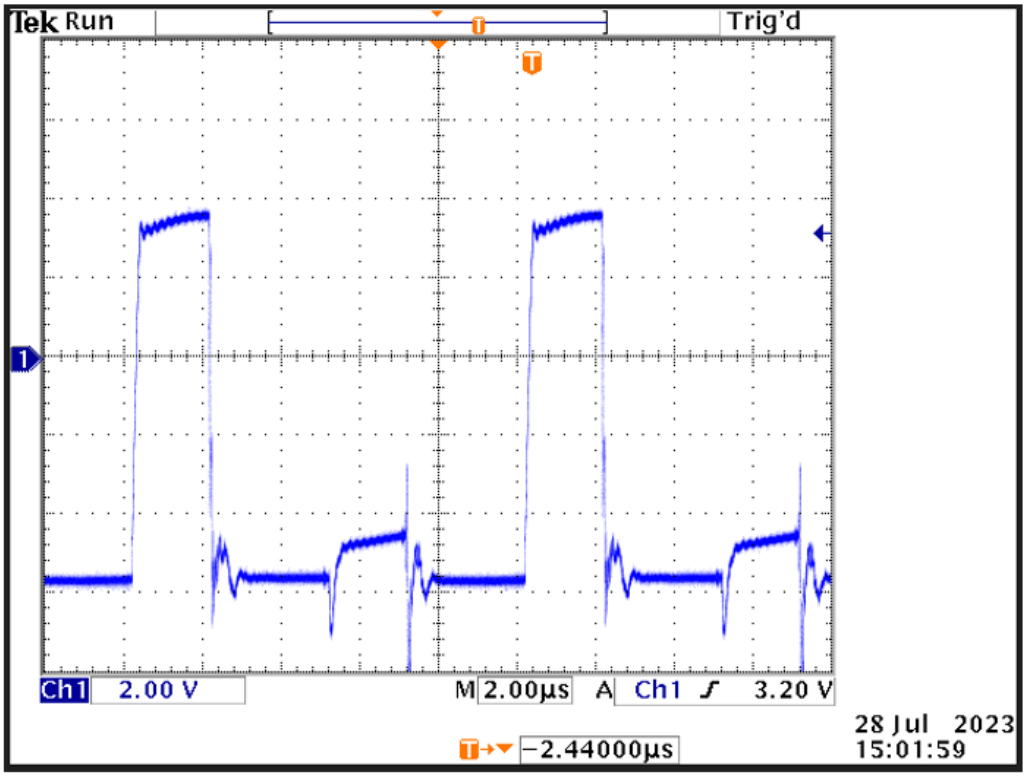

Figure 51: MOSFET's gate to source voltage

As it can be seen in the figures, the MOSFET is indeed commutating, however, noise can be observed, this is due the imperfect welding and parasite interferences.

5.1.2.3 Flying capacitor's voltage

5.1.2.3.1 Five percent o duty cycle

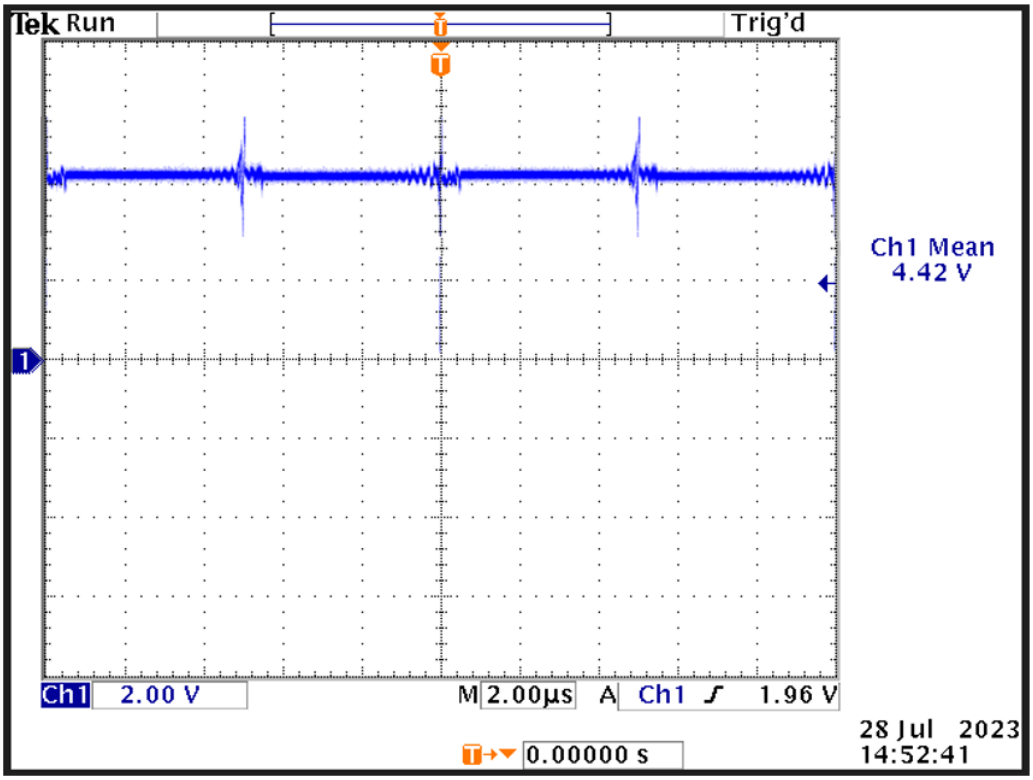

Figure 52: Flying capacitor's voltage

5.1.2.3.2 Ten percent of duty cycle

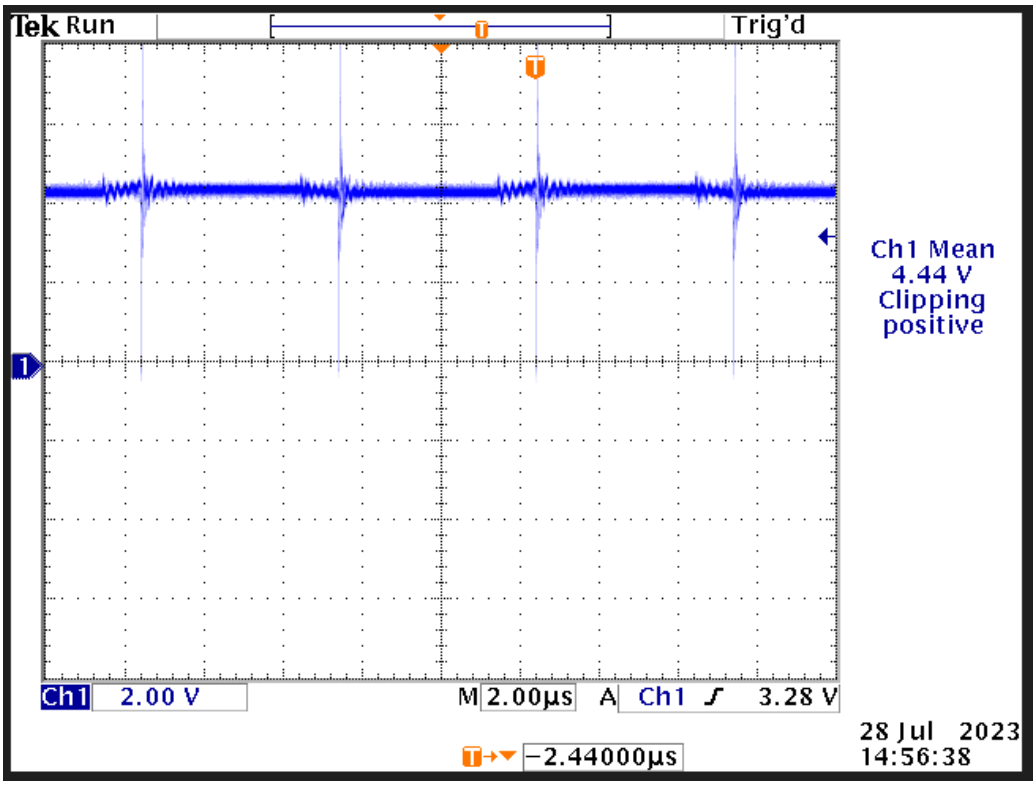

Figure 53: Flying capacitor's voltage

5.1.2.3.3 15% of duty cycle

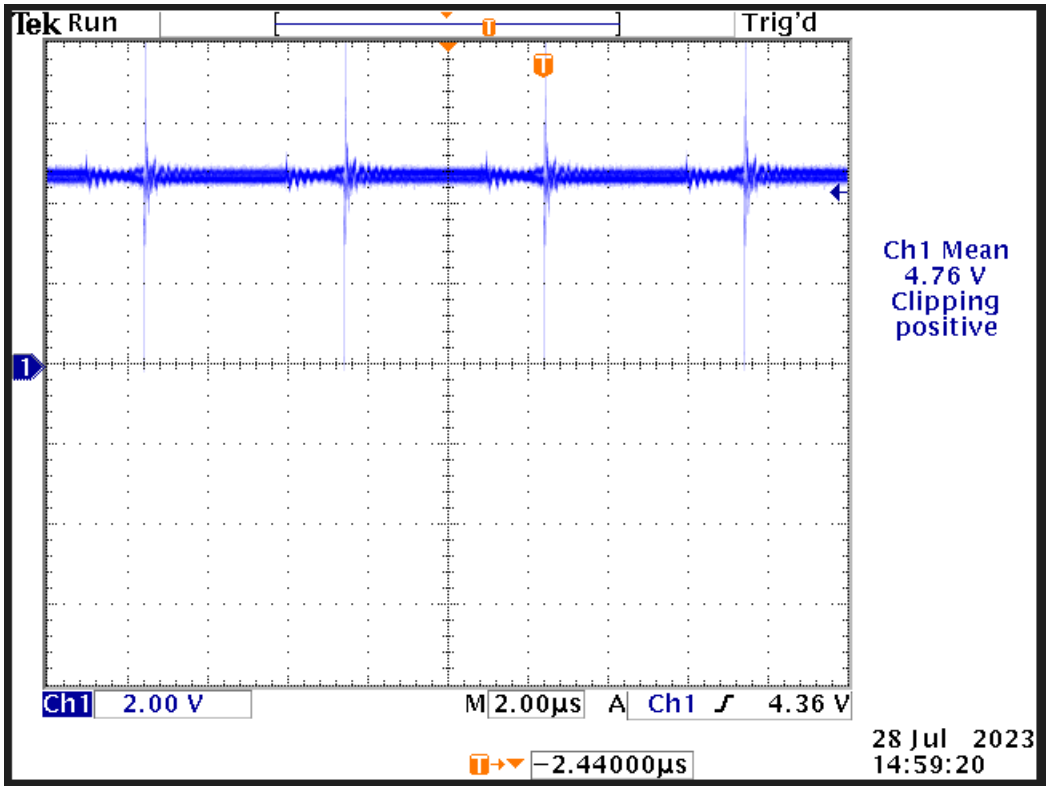

Figure 54: Flying capacitor's voltage.

5.1.2.3.4 Twenty percent of duty cycle

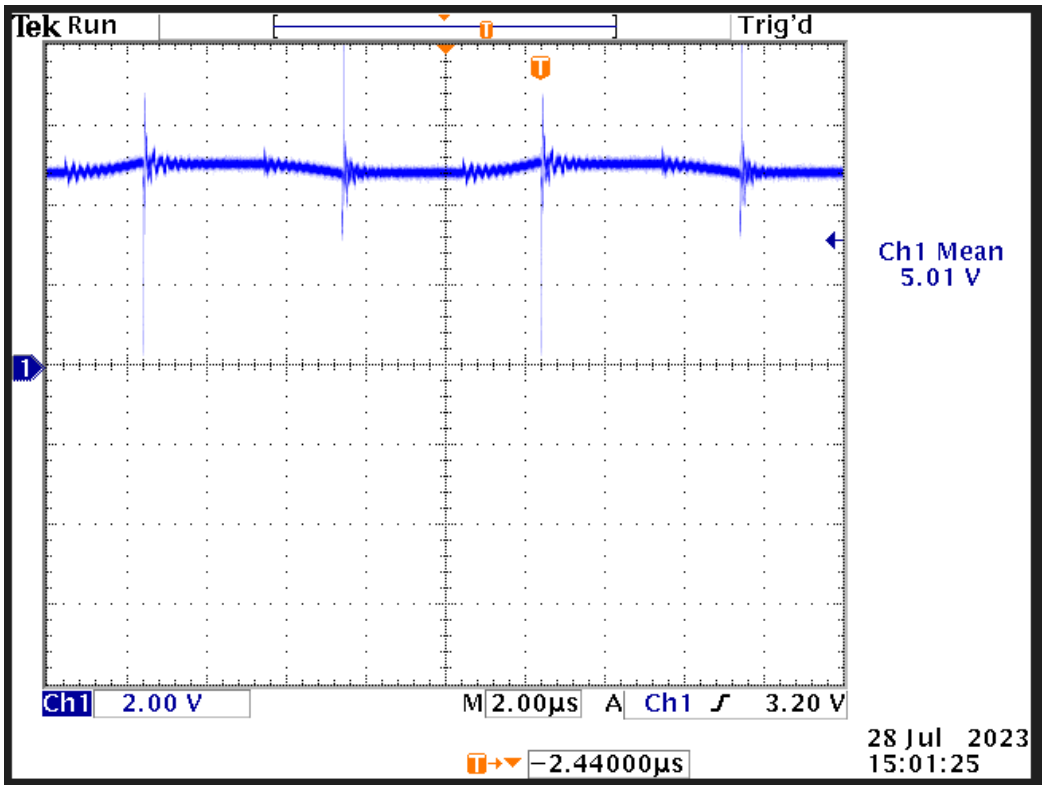

Figure 55: Flying capacitor's voltage.

As it can be seen in the figures the flying capacitor's voltage is quite stable even though it has some variations, it's true that looking at the different means it appears to be varying a lot, but this mean value is also affected by the noise. In the ideal converter, this voltage was 6 V which is different of the measured one, this is because the converter is not ideal and there were losses.

6. 3-level buck converter vs conventional buck converter

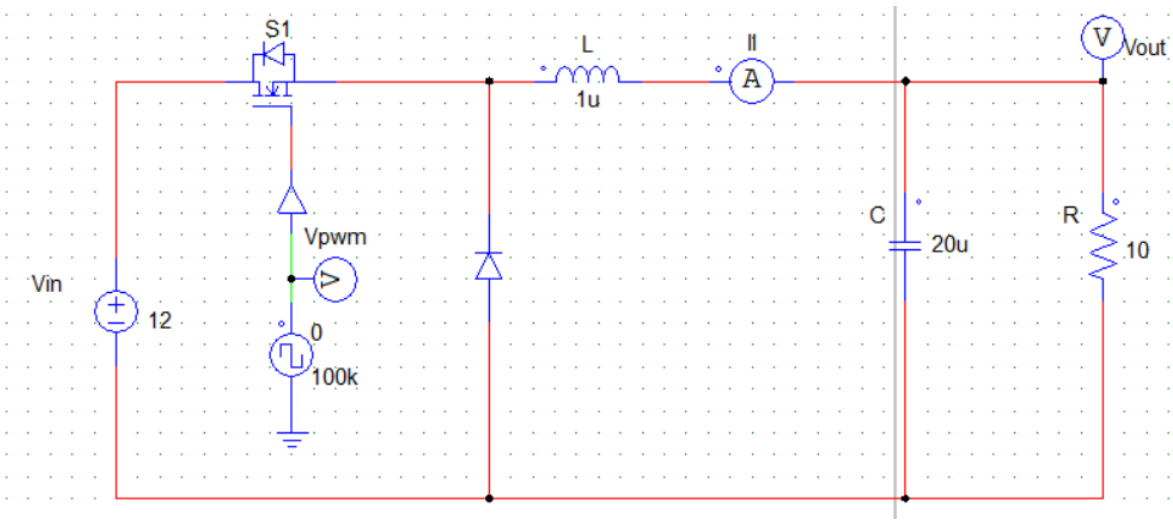

Figure 56: Conventional Buck converter

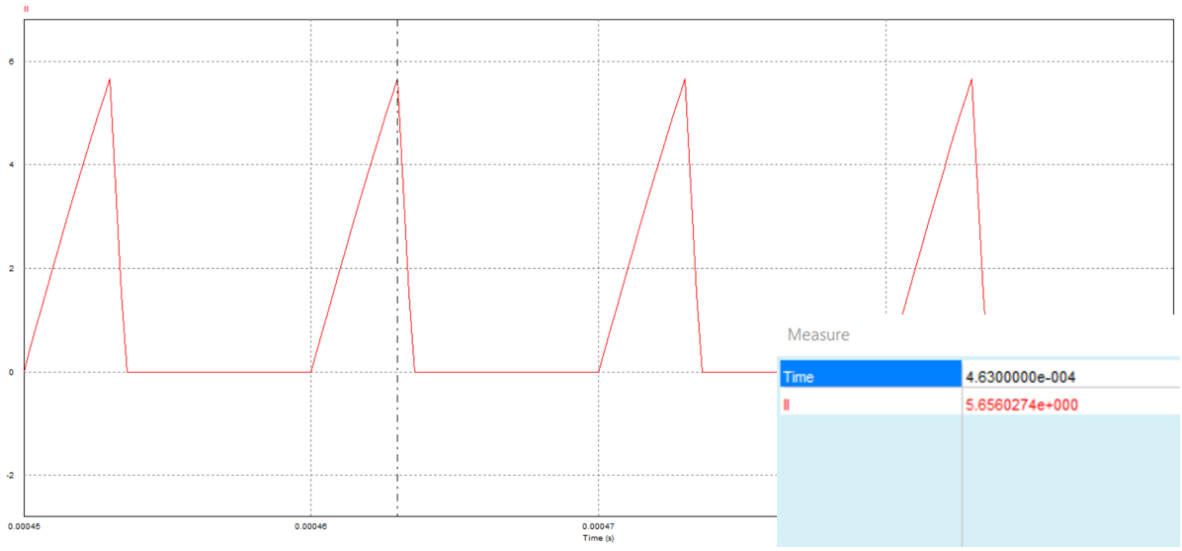

Figure 57: Conventional Buck converter inductor's peak current at a duty cycle of 30% (DCM).

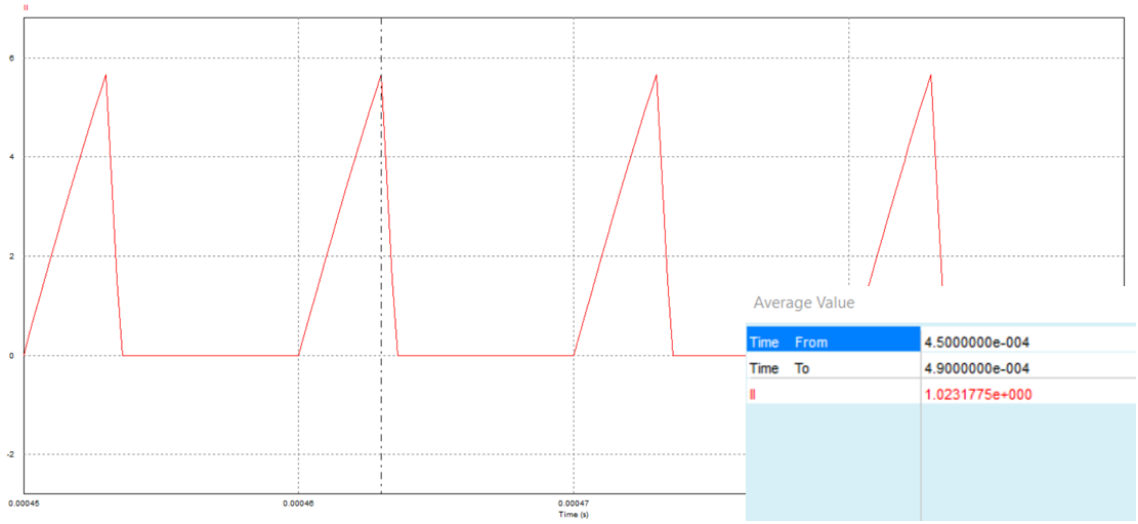

Figure 58: : Conventional Buck converter inductor's average current at a duty cycle of 30% (DCM).

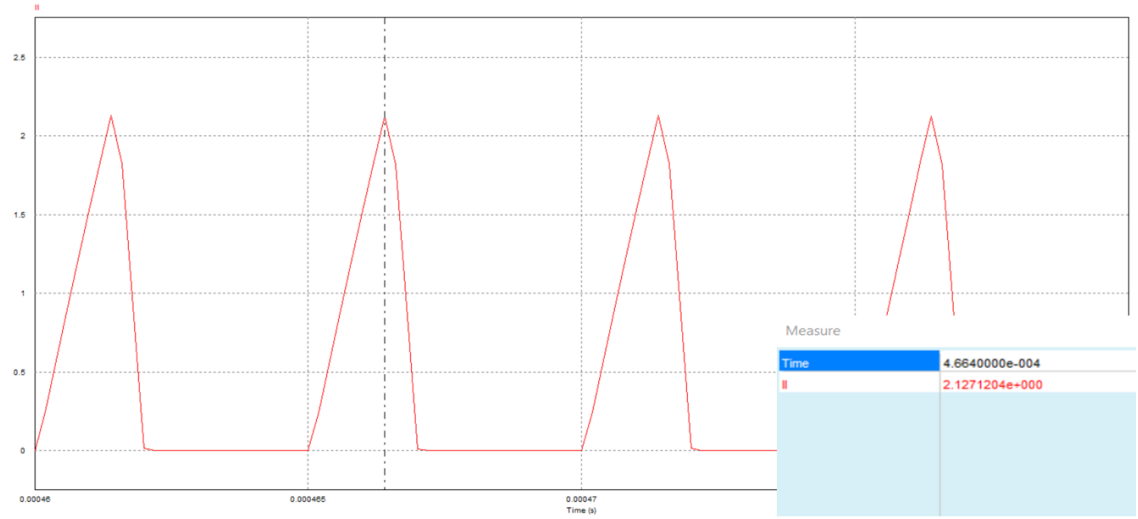

Figure 59: 3-level Buck converter inductor's peak current at a duty cycle of 15% (DCM).

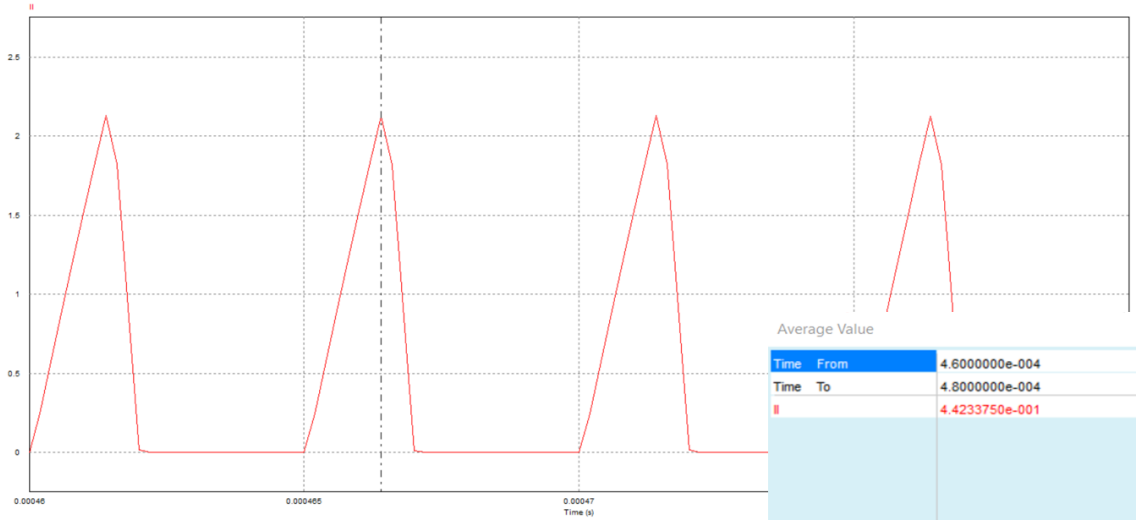

Figure 60: 3-level Buck inductor's average current at a duty cycle of 30% (DCM).

Table 4: Current comparison between the 3-level Buck converter and the conventional Buck converter

3-level Buck converter inductor's peak current	Conventional Buck converter inductor's peak current	3-level Buck converter inductor's average current	Conventional Buck converter inductor's average current
2.13 A	5.66 A	1.02 A	0.44 A

As it can be appreciated in Table 4, there is a significant decrease in the inductor's current in the 3-level Buck converter, since the load is the same for both converters, if the inductor's current is lower in the 3-level Buck converter, then the voltage across the filter's capacitor, will also be lower. It is proved that the inductor and capacitor will be faced to less stress and smaller replacements could be used (refer to expression (10) for a better understanding).

7. Conclusions

In summary, a steady state model has been obtained by studying the inductor current and the capacitor current in the different possible working states of the converter in the working conditions specified, a dynamic model has also been obtained by linearizing the expression involving the incremental parts of the variables, thanks to this model, a PI has been designed in order to obtained no steady state error but also achieving a 60º phase margin. Finally, a prototype has been build, specifically the power stage that has managed to work quite well, unfortunately it has not been possible to build the control due to time limiting factors, which is a shame since it would have been a great opportunity to see the dynamic performance in real life.

After a long mathematical and physical development, this 3-level buck converter has shown how having the same purpose as a conventional Buck converter, gives better results when talking about stress seen by the components. As when it comes to the mathematical models, it has been proving that by approach the analysis very similarly as it would have been done with a conventional converter, has given a correct and accurate behaviour, meaning that this kind of approach can be applied to a multilevel Buck converter containing more than three levels, therefore having the advantages mentioned in the introduction.

When it comes to the prototype, in general it had an expected behaviour, it's true that in some figures, different graph shapes have been observed when compared to the simulation, but the reasons have been stated, it's understandable that by doing this a converter in a matrix board with all the connections done by hand welding, there was going to be some limitations related to noise.

Looking at this project as a whole, it has been accomplished a very satisfying result even after facing all the problems along the way.

8. Annex

In this annex, there are the MATLAB scripts used to obtain the MATLAB figures that appear throughout this thesis.

```
26/07/23 16:47        D:\MATLABMARIO.m                          1 of 1

clc

R=10;
Vg=12;
Vc=2.34232921921325 ;
U=0.1;
T=5e-6;
C1=20e-6;
L=1e-6;

s=tf('s');

C=[0 1]

B=[Vg/(2*L)+(2*Vc^2)/(R*T*U^2*(Vg/2-Vc));0]

I=s*eye(2)

A_j=[(-2*Vc)/((Vg/2-Vc)*U*T) -Vc*Vg/(U*T*R*(Vg/2-Vc)^2); 1/C1 -1/(R*C1)]

Z=I-A_j

%%Modelo dinamico
Q=C*inv(Z)*B

bode (Q)

%%Convertidor
Gc=(35900*(s/7.83e+4+1))/(s)

%%Lazo abierto
T=Gc*Q

bode (T)
```

Figure 61: Script to obtain the bode plots and poles of the transfer function (38)

```
syms Vc Vg U T R L C1 s


C=[0 1]
```

```
C = 1×2
     0     1
```

```
B=[Vg/(2*L)+(2*Vc^2)/(R*T*U^2*(Vg/2-Vc));0]
```

B =

$$\begin{pmatrix} \frac{Vg}{2L} - \frac{2\,Vc^2}{RTU^2\left(Vc - \frac{Vg}{2}\right)} \\ 0 \end{pmatrix}$$

```
I=s*eye(2)
```

I =

$$\begin{pmatrix} s & 0 \\ 0 & s \end{pmatrix}$$

```
A_j=[(-2*Vc)/((Vg/2-Vc)*U*T) -Vc*Vg/(U*T*R*(Vg/2-Vc)^2); 1/C1 -1/(R*C1)]
```

A_j =

$$\begin{pmatrix} \frac{2\,Vc}{TU\left(Vc - \frac{Vg}{2}\right)} & -\frac{Vc\,Vg}{RTU\left(Vc - \frac{Vg}{2}\right)^2} \\ \frac{1}{C_1} & -\frac{1}{C_1 R} \end{pmatrix}$$

```
Z=I-A_j
```

Z =

$$\begin{pmatrix} s - \frac{2\,Vc}{TU\left(Vc - \frac{Vg}{2}\right)} & \frac{Vc\,Vg}{RTU\left(Vc - \frac{Vg}{2}\right)^2} \\ -\frac{1}{C_1} & s + \frac{1}{C_1 R} \end{pmatrix}$$

```
Q=C*inv(Z)*B
```

Q =

$$\frac{RTU\left(\frac{Vg}{2L} - \frac{2\,Vc^2}{RTU^2\left(Vc - \frac{Vg}{2}\right)}\right)(2\,Vc - Vg)^2}{8\,Vc\,Vg - 8\,Vc^2 - 8\,C_1 R\,Vc^2 s + 4\,TU\,Vc^2 s + TU\,Vg^2 s + 4\,C_1 R\,Vc\,Vg\,s - 4\,TU\,Vc\,Vg\,s + 4\,C_1 RTU\,Vc^2 s^2 + C_1 RTU\,Vg^2 s^2 - 4\,C_1 RTU\,Vc\,Vg\,s^2}$$

Figure 62: Script to obtain expression for the transfer function (38)

9. Acknowledgments

I would like to acknowledge the guidance, help and patience from my supervisor Dr Carlos Olalla, who has been present in all the mathematical development and has shared his knowledge in the laboratory to be able to make the prototype work.

I would also like to thank all the PhD students present in the laboratory for their help and their welcoming to their workspace where they made me feel like another team member.

Finally, I would like to thank all my family for giving me their support throughout all these years, especially my mother who has never doubted me and has always given me the motivation I needed to pursue my goals without caring how hard they are to be achieved, to my stepfather who has always given me guidance and has loved me like a son of his own, to my grandmother who has always been present, has blindly believed in me and has always prayed so everything to works out for me, to my step grandfathers that always remind me that nothing ever is as bad as it seems and to my father, even though he may not be with us I'm sure he's very proud of me.

10. References

[1] T. A. Meynard and H. Foch, "Multi-level conversion: high voltage choppers and voltage-source inverters," PESC '92 Record. 23rd Annual IEEE Power Electronics Specialists Conference, Toledo, Spain, 1992, pp. 397-403 vol.1, doi: 10.1109/PESC.1992.254717.

[2] L. Corradini and G. Bonanno, "Multi-level flying capacitor buck converters with digital-predictive current-mode control," 2021 (Università de Padova).

[3] Alexis Montes Passini Buck de 3 nivells amb condensador flotant en mode de conducció discontinua. (Treball de Fi de Grau. Universitat Rovira i Virgili)

[4] X. Liu, P. K. T. Mok, J. Jiang and W. -H. Ki, "Analysis and Design Considerations of Integrated 3-Level Buck Converters," in IEEE Transactions on Circuits and Systems I: Regular Papers, vol. 63, no. 5, pp. 671-682, May 2016, doi: 10.1109/TCSI.2016.2556098.

[5] Y. Yamauchi, T. Sai, T. Sakurai and M. Takamiya, "Modeling of 3-level buck converters in discontinuous conduction mode for stand-by mode power supply," 2017

IEEE International Symposium on Circuits and Systems (ISCAS), Baltimore, MD, USA, 2017, pp. 1-4, doi: 10.1109/ISCAS.2017.8050584

[6] L. F. Costa, S. A. Mussa and I. Barbi, "Multilevel buck dc-dc converter for high voltage application," 2012 10th IEEE/IAS International Conference on Industry Applications, Fortaleza, Brazil, 2012, pp. 1-8, doi: 10.1109/INDUSCON.2012.6453673.

[7] Olalla, Carlos & Queinnec, Isabelle & Leyva, Ramon. (2010). Robust linear control of DC-DC converters: A practical approach to the synthesis of robust controllers. (Universitat Politècnica de Catalunya)

[8] Jian Sun, D. M. Mitchell, M. F. Greuel, P. T. Krein and R. M. Bass, "Averaged modeling of PWM converters operating in discontinuous conduction mode," in IEEE Transactions on Power Electronics, vol. 16, no. 4, pp. 482-492, July 2001, doi: 10.1109/63.931052.